Atmos. Meas. Tech. Discuss., 6, 2353–2411, 2013
www.atmos-meas-tech-discuss.net/6/2353/2013/
doi:10.5194/amtd-6-2353-2013

Atmospheric Measurement Techniques Discussions
Open Access

Aerosol retrieval experiments in the ESA Aerosol_cci project

T. Holzer-Popp[1], G. de Leeuw[2,3,4], D. Martynenko[1], L. Klüser[1], S. Bevan[6], W. Davies[6], F. Ducos[5], J. L. Deuzé[5], R. G. Graigner[7], A. Heckel[6], W. von Hoyningen-Hüne[8], P. Kolmonen[2], P. Litvinov[5], P. North[6], C. A. Poulsen[7], D. Ramon[14], R. Siddans[9], L. Sogacheva[2], D. Tanre[5], G. E. Thomas[7], M. Vountas[8], J. Descloitres[10], J. Griesfeller[11], S. Kinne[12], M. Schulz[11], and S. Pinnock[13]

[1]Deutsches Zentrum für Luft- und Raumfahrt (DLR), Deutsches Fernerkundungsdatenzentrum, Oberpfaffenhofen, Germany
[2]Finnish Meteorological Institute (FMI), Helsinki, Finland
[3]University of Helsinki, Department of Physics, Helsinki, Finland
[4]TNO, Utrecht, The Netherlands
[5]Laboratoire d'Optique Atmosphérique, Lille, France
[6]Department of Geography, Swansea University, Swansea, UK
[7]Atmospheric, Oceanic and Planetary Physics, Department of Physics, University of Oxford, Oxford, UK
[8]Universität Bremen, Institute of Environmental Physics, Bremen, Germany
[9]Rutherford Appleton Laboratory (RAL), Space Science and Technology Department, Chilton, UK

[10]ICARE Data and Services Center, University of Lille, France
[11]Norwegian Meteorological Institute, Oslo, Norway
[12]Max-Planck-Institut für Meteorologie (MPI), Hamburg, Germany
[13]ESA, ESRIN, Frascati, Italy
[14]Hygeos, Lille, France

Received: 21 January 2013 – Accepted: 22 February 2013 – Published: 5 March 2013

Correspondence to: T. Holzer-Popp (thomas.holzer-popp@dlr.de)

Published by Copernicus Publications on behalf of the European Geosciences Union.

Abstract

Within the ESA Climate Change Initiative (CCI) project Aerosol_cci (2010–2013) algorithms for the production of long-term total column aerosol optical depth (AOD) datasets from European Earth Observation sensors are developed. Starting with eight existing pre-cursor algorithms three analysis steps are conducted to improve and qualify the algorithms: (1) a series of experiments applied to one month of global data to understand several major sensitivities to assumptions needed due to the ill-posed nature of the underlying inversion problem, (2) a round robin exercise of "best" versions of each of these algorithms (defined using the step 1 outcome) applied to four months of global data to identify mature algorithms, and (3) a comprehensive validation exercise applied to one complete year of global data produced by the algorithms selected as mature based on the round robin exercise. The algorithms tested included four using AATSR, three using MERIS and one using PARASOL.

This paper summarizes the first step. Three experiments were conducted to assess the potential impact of major assumptions in the various aerosol retrieval algorithms. In the first experiment a common set of four aerosol components was used to provide all algorithms with the same assumptions. The second experiment introduced an aerosol property climatology, derived from a combination of model and sun photometer observations, as a priori information in the retrievals on the occurrence of the common aerosol components and their mixing ratios. The third experiment assessed the impact of using a common nadir cloud mask for AATSR and MERIS algorithms in order to characterize the sensitivity to remaining cloud contamination in the retrievals against the baseline dataset versions. The impact of the algorithm changes was assessed for one month (September 2008) of data qualitatively by visible analysis of monthly mean AOD maps and quantitatively by comparing global daily gridded satellite data against daily average AERONET sun photometer observations for the different versions of each algorithm.

The analysis allowed an assessment of sensitivities of all algorithms which helped define the best algorithm version for the subsequent round robin exercise; all algorithms (except for MERIS) showed some, in parts significant, improvement. In particular, using common aerosol components and partly also a priori aerosol type climatology is beneficial. On the other hand the use of an AATSR-based common cloud mask meant a clear improvement (though with significant reduction of coverage) for the MERIS standard product, but not for the algorithms using AATSR.

1 Introduction

The IPCC has identified anthropogenic aerosols as the most uncertain climate forcing constituent (IPCC, 2007; GCOS-92, WMO, 2004), which calls for further work to improve all types of available observations. The satellite aerosol retrieval situation (even with most recent specific aerosol instruments) can be characterized as follows (see, e.g. Kokhanovsky and de Leeuw, 2009). The first algorithms worked with only one or two independent measurements (which required assumptions about all but the one retrieval parameter aerosol optical depth – AOD). The second generation of algorithms/instruments provide several independent observations (spectral, angular, polarization) to better limit the retrieval solution and reduce the number of a priori assumptions. Due to the non-linear, non-isotropic and non-homogeneous propagation of light through the earth-atmosphere system the sensitivity and thus the retrievable information is different for every different sensor/algorithm combination. These sensitivities depend on atmospheric aerosol load and its characteristics as well as properties of the underlying surface, the presence of clouds, the presence of trace gases and instrument characteristics such as spectral range, polarization and viewing angles. Therefore, products from different instruments cannot easily be compared or merged even if converted to a common reference wavelength. On the other hand the complementary sensitivities of different instruments hold the potential to increase the number of observations if used in a synergetic way.

AMTD
6, 2353–2411, 2013

The primary objective for the study described in this paper is to better understand and quantify the reasons for differences between the various aerosol products from the different algorithms and sensors described in Sect. 4. The assessment was based on a theoretical inter-comparison of the details of the different algorithm approaches. In order to quantify the influence of each assumption, several experiments were then carried out by producing global one month datasets from eight precursor algorithms with different prescribed aerosol properties and cloud masking.

Section 2 summarizes the analysis concept of Aerosol_cci. The common steps to improve and harmonize the algorithms are described in Sect. 3. These steps included the definition of common aerosol components and an aerosol type climatology, and the definition of a common nadir cloud mask. Section 4 describes the algorithms participating in the analysis and the specific implementation of the experiments for each of them. Section 5 gives an overview of the datasets produced, the evaluation tools used and the results of the experiments. The results are finally discussed in Sect. 6.

2 The analysis concept of Aerosol_cci

Within the ESA Climate Change Initiative (CCI, Hollmann et al., 2013) 13 Essential Climate Variables are under investigation, each of them in a dedicated project. Following GCOS principles each project started with a thorough analysis of user requirements and subsequently of available algorithms for producing consistent satellite-based long-term data sets. With regard to the aerosol variables, the project Aerosol_cci (July 2010–July 2013) brings together the major European aerosol retrieval experts and the AeroCom (aerosol model inter-comparison initiative) user community represented by its leaders. Aerosol_cci focuses on European total column aerosol optical depth (AOD) retrieval algorithms. In addition, also the OMI/SCIAMACHY absorbing aerosol index and GOMOS stratospheric extinction profiles are considered in the project (not analysed here, since they do not provide total AOD).

Discussion Paper | Discussion Paper | Discussion Paper | Discussion Paper |
AMTD
6, 2353–2411, 2013

The overall concept for the qualification of AOD algorithms in Aerosol_cci consists of three steps: (1) several algorithm experiments conducted on a minimal statistically significant amount of data in order to understand the effects of major assumptions (this paper); (2) a round robin exercise (four months, one in each season) to evaluate the improved algorithms versus a more comprehensive independent ground-based dataset and thus identify mature algorithms (de Leeuw et al., 2013) and finally (3) the production of a complete validated one year ECV product for assessment by the climate model community.

For the experiments, datasets covering the entire globe for one complete month (September 2008) were chosen as a compromise between statistical significance and production effort with eight algorithms and several experiments. The evaluation of the datasets was conducted by consideration of statistical parameters (mean bias, root mean square error – rmse, and Pearson correlation coefficient) attained from comparison of gridded 1° latitude longitude daily satellite products (level 3) versus AERONET daily averaged aerosol optical depth (AOD) interpolated to a reference wavelength at 0.55 µm. All experiments began with an analysis of baseline datasets for each algorithm (prior to making any changes).

In follow-up to the analysis discussed here, the round robin analysis (de Leeuw et al., 2013) included also assessment of satellite level 2 datasets (10 km super pixels) as well as inter-comparison to external reference datasets such as other satellite instruments (MODIS, MISR) or from models such as AeroCom median.

3 Common changes to the algorithms for the experiments

The algorithm development within Aerosol_cci was based on existing precursor algorithms with an initial focus on ENVISAT sensors and PARASOL with later extension to predecessor instruments (e.g. onboard ERS-2) and successor sensors (e.g. Sentinels). The key aerosol Essential Climate Variable (ECV) product of Aerosol_cci is global multi-spectral aerosol optical depth (AOD) and in addition information on aerosol type/aerosol optical properties, both including pixel-wise error information. The following three sub-sections describe the experiments conducted to study the sensitivity of the retrieval results to two of three most critical parts of aerosol retrieval algorithms: assumptions on aerosol optical properties and cloud masking. The third critical element, namely surface treatment, is typically intrinsic to each retrieval algorithm and thus was not (yet) assessed for all algorithms. For aerosol optical properties and cloud masking the ultimate goal was to come to harmonized definitions for a community algorithm.

3.1 Definition of common aerosol components

Aerosol size distributions in global modelling and satellite retrieval are commonly approximated by multi-modal log-normal number size distributions (Seinfeld and Pandis, 1998) covering a size range from a few nanometres to several tenths of micrometres:

$$\frac{\mathrm{d}N(r)}{\mathrm{d}\ln r} = \sum_{i=1}^{n} \frac{N_i}{(2\pi)^{1/2}\ln\sigma_i} \exp\left(-\frac{(\ln r_i - \ln \bar{r}_{\mathrm{g}i})^2}{2\ln^2\sigma_i}\right), \tag{1}$$

where each log-normal mode is defined by three parameters: aerosol number concentration N_i, number mode radius $\bar{r}_{\mathrm{g}i}$ and (geometric) standard deviation σ_i.

For use in satellite retrievals, only those particles need to be included that are large enough to be detected by optical instruments, i.e. with sizes larger than about 0.05 µm in radius. For those particles the scattering efficiency differs significantly from zero. Furthermore, because physical, chemical and optical properties of particles with radii smaller or larger than about 0.5 µm are usually quite different, the size distributions used in aerosol retrievals are usually described by a bi-modal distribution ($n = 2$ in Eq. 1). The two size modes are commonly referred to as the fine and coarse modes.

For the Aerosol_cci experiments the choices made for $\bar{r}_{\mathrm{g}i}$ and σ_i are presented for each size-mode in Table 1 (de Leeuw et al., 2013). These choices were based on probability distribution statistics derived from AERONET analysis, provided in Fig. 1, and detailed literature review of the various definitions currently in use in the eight

AMTD
6, 2353–2411, 2013

precursor and other aerosol retrieval algorithms. In basing these choices on AERONET statistics the authors are well aware of existing limitations (bi-modal size distribution, assumptions on refractive indices) but consider this dataset as the most comprehensive and uniform available source of aerosol property knowledge. Table 1 also provides the complex refractive indices used for the mid-visible region. The two fine mode types are taken as the two extremes in terms of absorption; the reality (in terms of absorption) is a combination of these two types. As can be seen in the joint probability distribution of the upper part of Fig. 1, based on AERONET sun photometer data, the most frequent fine mode size (in terms of the effective radius) is near 0.14 µm, which was thus chosen as characteristic value for the Aerosol_cci fine mode definitions shown in Table 1.

The coarse mode is dominated by two quite different aerosol types: spherical non-absorbing sea salt particles and non-spherical absorbing dust particles. Based on an AERONET probability distribution for the coarse mode shown in the lower part of Fig. 1, the effective radius was set to 1.94 µm for these two coarse mode aerosol types. Here it is noted that for sea salt aerosol the size distribution is slightly smaller to that recently derived by Sayer et al. (2012a), based on version 2 of the AERONET retrieval algorithm (Dubovik and King, 2000; Dubovik et al., 2006; Sinyuk, et al., 2007); Sayer et al. (2012a) derived an effective radius of 2 µm, a variance of 0.72 and a refractive index of (1.363, 3×10^{-9}). The assumed log-normal size mode is wider than the fine mode. However, it is noted that a small contribution of aerosol particles larger than 15 µm in radius cannot be ruled out. For dust the variability of effective radii between different regions is depicted in Fig. 2. Consequently, any definition adopted can only provide an average assumption and may differ from the reality in each specific retrieval case.

For the calculation of the aerosol optical properties for the aerosol types of Table 1, the particles are assumed spherical and a Mie code can be applied, except for dust for which aerosol is modeled as an ensemble of randomly oriented spheroids using the scattering kernels generated by Dubovik et al. (2006) using a combination T-matrix and improved geometrical optics calculations. The distribution of aspect ratios ranging between 1.44 and 3.0 was derived by Dubovik et al. (2006) by fitting phase matrices of

Discussion Paper | Discussion Paper | Discussion Paper | Discussion Paper |

AMTD
6, 2353–2411, 2013

Aerosol retrieval experiments in the ESA Aerosol_cci project

T. Holzer-Popp et al.

dust measured by Volten et al. (2001) in laboratory. Although spheroids may be unable to represent the entire shape complexity for dust, this spheroid method is preferable over methods for spheres. An important issue is also the choice of the correct refractive index for dust (Volten et al., 2001). Observational data (Dubovik et al., 2002; Sinyuk et al., 2003) demonstrate that the dust absorbing strength is spectrally dependent and decreases from the UV (refractive index near 0.005) to the near-IR (refractive index near 0.001).

All experiments described in this paper (except the baseline references) use this definition of four basic aerosol components, which are externally mixed or the mixing fractions even (partly) retrieved in a way specific by each algorithm.

3.2 Definition of a common aerosol component climatology

Having defined four common aerosol components for use in the retrieval algorithms (Table 1), the particular aerosol model applied to each retrieval pixel can then be determined by three external mixing fractions of AOD550 (aerosol optical depth at 0.55 µm, the usual mid-visible reference wavelength): the fine mode fraction of total AOD, the fraction of weakly absorbing fine mode AOD of total fine mode AOD, and the dust fraction of the coarse mode AOD.

The aerosol component experiments differ in the way these fractions were determined. In the first experiment algorithms tested a completely free retrieval of the three fractions and their associated AOD. In the second experiment, a priori information for these three fractions, all or in part (depending on capabilities of the different algorithms), based on climatological data was introduced. Since no global daily a priori maps of the aerosol type for 2008 are available a climatology was used. Such a climatology has been extracted from AeroCom model median global monthly maps (Kinne et al., 2006, Appendix) which were locally improved by using high quality statistics on the occurrence of aerosol components available from analysis of ground-based remote sensing from AERONET sun photometer network (Holben et al., 1998). Climatological data produced with this combination of AeroCom model and AERONET measurements

Discussion Paper | Discussion Paper | Discussion Paper | Discussion Paper |

AMTD

6, 2353–2411, 2013

Aerosol retrieval experiments in the ESA Aerosol_cci project

T. Holzer-Popp et al.

Title Page
Abstract Introduction
Conclusions References
Tables Figures
Back Close
Full Screen / Esc
Printer-friendly Version
Interactive Discussion

for the month of September for the three mixing fractions (and for reference the total AOD) are presented in Fig. 3. In order to demonstrate the implementation of the common aerosol model in the retrieval algorithms, this figure does not show parameters such as single scattering albedo, but rather the three mixing fractions used in the retrievals.

3.3 Selection of a common cloud mask

Reliable cloud masking is an essential part of aerosol remote sensing algorithms as cloud contamination can significantly increase measured reflected radiance and thus retrieved AOD. In recent years also the radiative transfer in the vicinity of clouds came into discussion, as it is not as straightforward to detect cloud contaminated pixels as it may seem (Koren et al., 2007, 2008). Especially for satellite observations with spatial resolution in the order of 1 km this may result in significant misinterpretation (Koren et al., 2008; Coakley et al., 2005). Thus cloud masking has to take into account also some “twilight” or “safety” zone around clouds to reduce impacts of three-dimensional effects or contamination from sub-pixel clouds on aerosol retrievals.

Cloud masking is an application of satellite remote sensing with a long history, but nevertheless cloud information for different applications (such as cloud properties, atmospheric sounding, aerosol or sea surface remote sensing, vegetation and land surface observations) has different requirements on cloud detection schemes. Most cloud detection techniques use similar physical principles, but there are large differences in thresholds defined in accordance with the intended application. Consequently, cloud masking results differ, even when applied to the same sensor.

For the third experiment a common cloud mask had to be identified for use in all participating aerosol retrieval algorithms. In order to choose a well performing cloud mask with a reasonable effort, a set of 17 globally distributed scenes from four different days of September 2008 (1, 6, 7, and 25) was selected for inter-comparison of the nadir cloud masks used in the different precursor algorithms. These scenes covered the most difficult conditions (in terms of aerosol remote sensing) with different types of

AMTD
6, 2353–2411, 2013

clouds and partly coincident high aerosol loadings (heavy smoke plumes from biomass burning, airborne dust transported over the ocean, industrial haze). Visual identification of obvious cloud and aerosol patterns in true colour composite images from the MODerate resolution Imaging Spectro-radiometer (MODIS) was used as additional independent comparison due to its better visualisation of aerosol plumes.

An example result of one single scene analysis is shown in Fig. 4 for 1 September 2008 east off the coast of Madagascar. True colour RGB images from AATSR (left) and MODIS-Terra (right) show the main cloud-aerosol features from south to north: optically thick strati-form clouds, an east-west cirrus band, an east-west aerosol plume (only visible in MODIS), and north-south bands of convective clouds. Between the two true colour images cloud masks are shown from left to right: a composite of AATSR APOLLO (AVHRR Processing scheme Over Land, cLouds and Ocean, used in SYNAER) and ESA operational (as used in ORAC and SU algorithms) cloud masks, an ADV AATSR cloud mask and the MERIS ESA operational cloud mask. No effort was made to use common projections and visualisations, as the main differences became visible even with a qualitative analysis of images as provided by the respective partners.

It is evident in Fig. 4 that all AATSR cloud mask are able to detect the main cloud features well, but the three AATSR nadir cloud masks are not identical. The cloud fraction estimated by the ESA operational AATSR mask is generally much higher than from APOLLO leaving fewer observations for aerosol retrieval (higher sensitivity near cloud edges, classification of structured land surfaces as clouds, artificial patterns arising over ocean). Part of the smoke plume (shown in the MODIS RGB image) and is flagged as cloudy by it. On the other hand, the ESA operational mask partly fails to detect shallow inland convection. The ADV AATSR mask misses part of the cirrus band. The MERIS standard algorithm cloud flag widely fails to detect the cirrus cloud band due to the lack of TIR channels.

The analysis of all 17 scenes (not shown) led to following overall outcome: the ESA operational AATSR mask fails to detect a substantial amount of closed large scale

AMTD
6, 2353–2411, 2013

stratocumulus fields with high reflectance. APOLLO and to some extent also the ESA operational AATSR cloud mask classify inland water bodies and river estuary regions with high amount of dissolved particles or shallow water as cloudy. For heavy dust events APOLLO and the ESA operational AATSR mask frequently fail to distinguish between dust and cloud. The ESA operational AATSR cloud mask fails to detect part of the shallow (scattered) clouds with warm tops. The FMI AATSR cloud mask misses part of the cirrus cloud cover. Potential high-reaching biomass burning plumes are classified as cloudy by all masks. The MERIS standard algorithm cloud flag has generally lower cloud fraction compared to all AATSR masks and it partly fails to detect scattered (strato-) cumulus clouds within dust plumes.

After evaluating the strengths and limitations of the different cloud masks used in the precursor algorithms on the 17 test scenes, it was agreed to use the APOLLO cloud mask as common nadir cloud mask for the third experiment. The safety zone was set to a 10 km surrounding of cloudy pixels (which means a highly conservative experiment to be sure to avoid any cloud contamination). Evidently, also APOLLO cannot provide a perfect cloud mask and further work is needed to explore opportunities for its optimization.

The APOLLO scheme is based on a variety of different tests with solar and thermal channels including reflectance ratios, brightness temperature differences and histogram tests. The method was originally developed by Saunders and Kriebel (1988) and re-evaluated and updated by Kriebel et al. (2003) for the AVHRR operated on the NOAA satellite series. The APOLLO algorithm has also been transferred to a set of other satellite sensors including AATSR onboard ENVISAT. For application in the field of aerosol retrieval, another set of updates to the AATSR adaptation of APOLLO was described in Holzer-Popp et al. (2008).

As illustration of spatial aerosol retrieval limitations in the experiments conducted Fig. 5 presents the global monthly mean cloud fraction for September 2008 obtained from the APOLLO method with AATSR. It is evident that over ocean the cloud fraction is generally higher than over land, especially in the subtropical subsidence regions and

AMTD

6, 2353–2411, 2013

only few regions over land have more than 60 % cloud-free observations. This common nadir cloud mask was used with the native AATSR orbit pixel 1 km resolution in the third experiment of Aerosol_cci for the retrievals using ENVISAT morning observations (AATSR, MERIS, synergetic AATSR+SCIAMACHY); it could not be directly transferred to the afternoon PARASOL data due to the large temporal variability of clouds.

4 Algorithms participating in the analysis

The initial focus of Aerosol_cci was on ENVISAT instrumentation (AATSR, MERIS, SCIAMACHY), which have well cross-calibrated visible reflectance to within a few percent and in order to avoid miss-time and miss-distance issues when inter-comparing their products. One additional European instrument assessed was PARASOL due to its very high information content of its multi-spectral, multi-angular and polarization measurements. The precursor algorithms which provide total column aerosol optical depth and were included in the experiments are listed in Table 2. For each algorithm the major principles, capabilities and limitations as well as the specific way of implementing the experiments are briefly discussed in the following sub sections (referring to literature for more details).

4.1 The FMI AATSR retrieval (ADV/ASV)

The AATSR dual-view (ADV) algorithm for the retrieval of optical properties of aerosols over land utilizing the AATSR/ATSR-2 top-of-atmosphere (TOA) reflectances is described in, e.g. Veefkind et al. (1998) and Kolmonen et al. (2013). Retrievals are only made for cloud-free scenes; the cloud screening method is described in Curier et al. (2009). The AATSR/ATSR-2 instruments have two views: forward and near-nadir. These two views are used in the treatment of the ground reflectance based on the so-called k-assumption where the ratio (k) of the ground reflectances for the two views is assumed to be independent of wavelength (Flowerdew and Haigh, 1995). The k-ratio

AMTD
6, 2353–2411, 2013

is computed at the 1.61 µm wavelength, where reflectance due to aerosols is in first approximation assumed to be negligible compared to ground reflectance. In the retrieval, the aerosol is described as a mixture of two components (baseline algorithm, see Sect. 3.1 for use of aerosol models in the cci project). The mixing ratio is iterated to best match the reflectances measured by the AATSR/ATSR-2 instrument at the top of the atmosphere, at all of the available wavelengths (0.555, 0659 and 1.61 µm) together. The mixing ratio corresponds to the fine-mode fraction.

Over ocean only the forward view is used for aerosol retrieval, because of the longer atmospheric path length and thus higher sensitivity to aerosols. The aerosol single view (ASV) algorithm minimizes the discrepancy between the TOA-measured and the modelled reflectances (using the DAK radiative transfer model) at the wavelengths of 0.555, 0.659, 0865 and 1.61 µm (Veefkind et al., 1998). The modelled reflectances include the ocean surface contributions from specular (Fresnel) reflectance and reflectances caused by chlorophyll and whitecaps. Sun-glint contaminated pixels are excluded from the retrieval. As in ADV, the aerosol model used is a mixture of two aerosol components (baseline algorithm).

The latest versions of ADV and ASV are described in Kolmonen et al. (2013). The products include AOD at 3 (4 over ocean) wavelengths, Ångström exponent and mixing ratio. Single scattering albedo and land surface reflectance are currently being validated. For the retrieved AOD pixel level uncertainty was determined by progressing the measurement error of TOA reflectance through the retrieval process.

The aerosol climatology within Aerosol_cci was implemented in three different ways. First, the fine-mode fraction, the mixture between absorbing/non-absorbing fine particles, and the dust fraction were used without modifications in the retrieval. Second, the fine-mode fraction was retrieved. Third, the fine-mode fraction and the mixture between absorbing/non-absorbing fine particles were retrieved. All mixtures were treated as external ones. This version is more complex when compared to the baseline algorithm because one new mixture is introduced. The fine-mode fraction was converted to the above mentioned mixing ratio during retrieval.

For the cloud mask experiments described in this paper, the Aerosol_cci cloud mask was collocated in the algorithm and used instead of the default ADV/ASV cloud screening. All the different aerosol climatology schemes were also used for the retrievals together with the cloud mask. The retrieval part of the algorithm was unchanged from that described above. In all other experiments the default cloud mask was used.

4.2 The Oxford RAL Aerosol and Cloud retrieval (ORAC)

The term ORAC describes an optimal estimation retrieval scheme designed for the retrieval of aerosol and/or cloud properties from visible-infrared imaging satellite radiometers. In different guises it has been applied to a number of different instruments to produce a range of different aerosol and cloud products. These include the Global Retrieval of ATSR Cloud Parameters and Evaluation (GRAPE) project (Sayer et al., 2012b; Thomas et al., 2010), where it was applied to the second and third Along-Track Scanning Radiometer instruments (ATSR-2 and Advanced-ATSR) to provide both cloud and aerosol properties from 1995–2010; the ESA GlobAEROSOL project, where it formed the basis of ATSR-2, AATSR and Spinning Enhanced Visible-InfraRed Imager (SEVIRI) aerosol products; and it is now involved in both the ESA Aerosol_cci and Cloud_cci projects (where it is being applied to MODIS, AVHRR and AATSR radiances). For a detailed description of the various versions of the ORAC aerosol retrieval the reader is referred to Thomas et al. (2009), while the details of the cloud retrieval are discussed by Poulsen et al. (2012).

The version of ORAC which is being used in the Aerosol_cci algorithm evaluation is an aerosol only retrieval which is intended for application specifically to the (A)ATSR instruments (as well as the upcoming Sea and Land Surface Temperature Radiometer that will form part of the European Sentinel series satellites).

Based on an optimal estimation retrieval framework (Rodgers, 2000), providing rigorous uncertainty propagation (providing pixel-by-pixel uncertainty on retrieved quantities) and inclusion of a priori knowledge, the optimal estimation approach ensures that

AMTD
6, 2353–2411, 2013

the most is made of the information provided by the measurements, by calculating all retrieved parameters as a function of all measurements simultaneously.

A forward model is used based on the BRDF description of the surface reflectance, allowing the dual-view capabilities of (A)ATSR to be fully exploited over land and ocean. Radiative transfer forward modelling is based on DIScrete Ordinates Radiative Transfer (DISORT – Stamnes et al., 1988), which includes multiple scattering between externally-mixed aerosol components, background atmosphere and surface. This provides accurate radiative transfer for all atmospheric conditions from completely clear to highly turbid.

Retrieval of AOD, aerosol effective radius (through alteration of the mixing state of the aerosol) and surface reflectance at each measurement channel (0.55, 0.67, 0.87 and 1.6 µm) are conducted. Surface reflectance is retrieved as a bi-hemispherical reflectance, with the directional dependence of the BRDF being constrained by a priori values. These are provided by the MODIS MCD43B surface BRDF product over land (Sayer et al., 2011) and a comprehensive sea-surface reflectance model (Sayer et al., 2010) over ocean.

In its baseline form (i.e. the configuration before the beginning of the Aerosol_cci project) ORAC used selection aerosol classes based on the Optical Properties of Aerosol and Cloud (OPAC) database (Hess et al., 1998) and from the work of Dubovik et al. (2002). These classes consist of external mixtures of between two and four log-normally distributed aerosol modes of different sizes. In ORAC the mixing ratio of the different size modes within each aerosol class – as parameterised by the aerosol effective radius – is a free parameter, which allows a wide range of aerosol properties to be modelled using a relatively small number of distinct classes. The baseline ORAC product was produced using classes based on the "continental clean", "maritime clean" and "desert dust" OPAC classes, with the addition of a South American cerrado biomass burning class based on Dubovik et al. (2002).

Incorporating the Aerosol_cci common aerosol models into ORAC was achieved by producing a total of ten new aerosol classes based on the climatology presented in

AMTD
6, 2353–2411, 2013

Fig. 3, which represent the full range of fine-mode absorbing/non-absorption ratios and dust/sea salt ratios found in the climatology. For the "free retrieval" ORAC product, the aerosol class for each retrieved pixel was selected based on a chi-squared goodness of fit measure. For the prescribed aerosol type product, the class was selected to match the climatology, although course-fine mode ratio was still free to vary (as the effective radius remains a retrieval parameter).

ORAC cloud masking is based on the ESA operational AATSR cloud flag, with additional tests to address known problems with it. In particular, an additional NDVI based test (in both forward and nadir views) is used to remove low, warm clouds over ocean and pixels which are saturated in the shortwave bands (and are often flagged as clear) are also accounted for. Additionally, a spatial homogeneity test is performed to detect sub-pixel clouds and desert dust, volcanic ash and biomass burning flags are applied to correctly identify dense aerosol plumes. Versions of the ORAC product were also produced using the APOLLO based common cloud mask, rather than the native ORAC mask. However, this resulted in a significant decrease in the quality of the product, which was found to be due to a bug in the implementation of this version. Thus the respective experiment is not included in this paper.

4.3 The Swansea University AATSR retrieval (SU)

The algorithm is based on iterative optimization subject to multiple constraints, and is documented in the papers (North et al., 1999; North 2002; Grey et al., 2006a,b; Bevan et al., 2012). Over land the method is based on a multi-angular constraint, and over ocean a spectral constraint; both use the dual-viewing capability of the AATSR instrument. The algorithm has two steps: (1) given a set of satellite TOA radiances, and an initial guess of atmospheric profile, the corresponding set of surface reflectances is estimated. (2) Application of the constraint set to this set of reflectances results in an error metric, where a low value of this metric should correspond to a set of surface reflectances (and hence atmospheric profile) which is realistic. Step (1) is repeated with a refined atmospheric profile until convergence at an optimal solution, retrieving

Discussion Paper | Discussion Paper | Discussion Paper | Discussion Paper |

AMTD

6, 2353–2411, 2013

both aerosol model and optical depth. The uncertainty in the retrieved AOD is derived from the curvature of the error surface near the minimum, and per-channel instrument and surface model uncertainties. The main elements therefore are (i) an efficient and accurate LUT scheme for deriving surface reflectance for known atmospheric profile, and (ii) formulation of constraints on the land or ocean surface reflectance suitable for inversion (Smith, 2005).

For computational efficiency a set of pre-calculated look-up tables (LUTs) is employed which map top-of-atmosphere reflectance to surface reflectance for a range of surface and atmospheric conditions. For the current operational implementation used to derive global aerosol, the lookup tables of atmospheric properties for the algorithm are generated using the forward simulations of 6S atmospheric radiative transfer code model (version 4.1, Vermote et al., 1997). Correction for water vapour and ozone, as well as coupling effects, such as multiple land-atmosphere scattering, are implicitly represented in the LUTs. The retrieval of aerosol properties is normally made at a coarser grid than the sensor resolution, to allow computational efficiency and to minimise registration error. In the operational implementation, aerosol models used are those defined within the 6S code. Surface pressure, ozone and water vapour are estimated from best available ancillary data (ECWMF fields).

The purpose of surface constraints are to define an error metric derived from the surface reflectance, which then allow iterative estimation of best-fit AOD and aerosol model. Over land this is based on the angular variation of reflectance, while over ocean the spectral variation is constrained. For the ATSR series, the ratio of surface reflectances at the nadir and forward viewing angles is well correlated across wavebands, and the variation in anisotropy may be modeled simply (Veefkind et al., 1998; North et al., 1999). This avoids the need for assumptions on absolute surface brightness or spectral properties. The method differs from other approaches by using a more sophisticated physically based surface model to account for spectral variation of the surface anisotropy owing to the variation of the fraction of scattered light with wavelength (North et al., 1999).

AMTD
6, 2353–2411, 2013

The Swansea University retrieval algorithm has been applied to both ATSR-2 and AATSR dual-view observations, and is employed to generate a global dataset for the AATSR instrument under the ESA GPOD system. It also forms the basis of aerosol retrieval under the ESA MERIS/AATSR Synergy project, and is developed for implementation under the GMES Sentinel-3 Synergy processing chain. The framework is also used for atmospheric correction for the ESA GlobAlbedo project. The full 13-yr ATSR-2/AATSR data series has been processed on ESA GPOD and evaluated against AERONET for selected regions (Bevan et al., 2009, 2012).

The ESA GPOD dataset was used to provide the Aerosol_cci baseline product. For the subsequent Aerosol_cci experiments the atmospheric LUT set was replaced by a new set of LUTs derived using the common aerosol model definition for four pure components. For experiment 1, the best fitting pure component model was returned without a priori assumptions. For experiment 2, a larger LUT based on 35 external mixtures of these components was derived, and estimation of continuous component fractions defined by local climatology was estimated by tetrahedral interpolation of radiative components. The climatology model was used as an a priori estimate of aerosol type, and retrieval proceeded using this in addition to a fixed set of mixtures. Best model was chosen based on optimisation as before, with weighting of the error function parameterised to favour the climatology model and to force the retrieved model to the climatology for low AOD (< 0.2) where constraint from the data is weak. The APOLLO common cloud mask (experiment 3) including safety zone was implemented for nadir viewing; however the original cloud mask was used to further screen cloud in the forward view since a common forward cloud mask was not defined.

4.4 The synergetic aerosol retrieval for AATSR and SCIAMACHY (SYNAER)

The synergistic aerosol retrieval method SYNAER delivers aerosol optical depth (AOD) and an estimation of the type of aerosols in the lower troposphere over both land and ocean by exploiting a combination of a radiometer (e.g. AATSR) and a spectrometer (e.g. SCIAMACHY). In retrieving AOD the free tropospheric and stratospheric aerosol

AMTD
6, 2353–2411, 2013

concentration are kept constant at background conditions, whereas the boundary layer aerosol concentration and type and a possible dust layer are varied. The type of aerosol is estimated as a percentage contribution of representative components from an extension of the OPAC (Optical Parameters of Aerosols and Clouds; Hess et al., 1998) dataset to AOD in the boundary layer. The high spatial resolution including thermal spectral bands of the radiometer permits accurate cloud detection. The SYNAER aerosol retrieval algorithm comprises then of two major parts: (1) in step 1 a dark field method exploits single wavelength radiometer reflectances (at 0.67 µm over land, at 0.87 µm over ocean) to determine 40 values of the aerosol optical depth over automatically selected and characterized dark pixels both for a set of 40 different pre-defined boundary layer aerosol mixtures. Then, using AOD interpolated between nearby dark pixels the surface reflectance of every radiometer pixel is retrieved for the same set of aerosol mixtures. (2) In step 2 the parameters retrieved in the first step are used to simulate spectra for the same set of 40 different aerosol mixtures with the same radiative transfer code after spatial integration to the larger pixels of the spectrometer. A least square fit of these calculated spectra at 10 wavelengths to the measured spectrum delivers the correct AOD value (the one AOD retrieved in step 1 for the aerosol type selected in step 2) and – if a uniqueness test is passed – the most plausible spectrum and its underlying aerosol mixture. The entire method uses the same aerosol model of basic aerosol components, each of them representing optically similar aerosol species. These basic components are externally mixed into 40 different aerosol types covering a realistic range of atmospheric aerosol masses. Also the underlying radiative transfer code (SOS; Nagel et al., 1978; extended after Popp, 2005) is consistently used throughout all retrieval steps. (Holzer-Popp et al., 2002, 2008).

In Aerosol_cci the four common optical components were used to define a set of 36 aerosol mixtures covering a realistic range of atmospheric aerosol conditions. Radiative transfer look-up tables were then calculated and used for a free retrieval of AOD together with all three mixing fractions. Also, the AeroCom/AERONET climatology was

AMTD
6, 2353–2411, 2013

used to identify the nearest discrete mixture along the three mixing fractions and use the respective look-up table for each retrieval pixel.

Since SYNAER uses the DLR APOLLO cloud mask, the experiment on the common cloud mask was of limited scope for SYNAER. However, the different size of the safety zone (5 km for SYNAER baseline and 10 km for the common cloud mask) was tested in the third experiment. As the nadir only approach of SYNAER (adopted for consistency with successor instruments AVHRR+GOME-2 onboard METOP) makes the surface brightness parameterization important, an experiment was conducted for this algorithm only (not shown here), where the surface albedo of all retrieval pixels was reduced by 0.01 at the retrieval wavelengths of 0.67 µm (over land) and of 0.87 µm (over ocean).

The specific focus of SYNAER is the estimation of the aerosol type, which is not in the focus of the analysis in this paper. However, it could be shown, that the use of the new optical aerosol components leads to a qualitative improvement of the retrieved global AOD patterns of the individual components; this will be evaluated quantitatively and summarized in a separate paper.

4.5 The Bremen Aerosol retrieval for MERIS (BAER)

For the determination of AOD from observation of the MERIS single-view multi-spectral imager the Bremen AErosol Retrieval algorithm (BAER) (von Hoyningen-Huene et al., 2003, 2006) was used. The basis is the solution of the radiative transfer equation for the aerosol reflectance. Aerosol reflectance is obtained by subtracting Rayleigh path reflectance for the given illumination and viewing geometry and the appropriate pressure conditions and correcting for the surface term. The determination of Rayleigh path reflectance uses a digital elevation model (GTOPO30) for the estimation of the height variation of the atmospheric pressure.

Over land the variable surface albedo is considered by a mixing model of surface reflectance, yielding it as fractions of "green vegetation" and "bare soil". This model is tuned by two parameters estimated from the satellite scene itself, namely the vegetation fraction as a function of normalized differential vegetation index, and a reflectance ratio to adjust the absolute value of the reflectance in the retrieval channel at 0.67 µm. For the surface albedo BRDF effects are considered, using the Raman-Pinty-Verstraete model (Maignan et al., 2004).

Over ocean a similar mixing model is used, tuning water leaving reflectance by mixing of a clean ocean spectrum with one of coastal water. The tuning uses the NDPI (normalized differential pigment index). The Fresnel reflectance of the water surface is modelled, using Cox and Munk (1954).

Finally look-up-tables for a selected aerosol type are used to estimate AOD. The LUTs are obtained by radiative transfer modelling of aerosol reflectance for given geometry conditions, a range of AOD values, phase function of a selected aerosol type, single scattering albedo and surface albedo. The described procedure yields the spectral AOD for the short-wave channels of MERIS (channels 1–7, 0.412–0.665 µm) on a pixel-by-pixel basis.

So far, BAER has not yet been adapted to the common cloud mask due to technical constraints, but the common aerosol optical components in Aerosol_cci have been implemented with a limited number of fixed mixtures of them.

4.6 The ESA MERIS standard retrieval

The MERIS standard aerosol retrieval over land algorithm was originally designed to work over Dense Dark Vegetation (DDV) targets (Santer et al., 1999, Ramon and Santer, 2001). A set of DDV Bidirectional Reflectance Function (BRF) models was assembled for 11 different biomes on Earth. DDV detection is based on a threshold on the Atmospherically Resistant Vegetation Index (ARVI) computed from Rayleigh corrected reflectances at 0.443, 0.665 and 0.865 µm. As DDV spatial cover is low, the aerosol inversion was extended to brighter surfaces called Land Aerosol Remote Sensing (LARS) targets (Santer et al., 2007). LARS spectral albedo can be predicted as it is linearly related to ARVI. Slopes and offsets of these linear regressions are stored in look-up tables for $1^\circ \times 1^\circ$ boxes and on a monthly basis. The aerosol retrieval consists in the inversion of the AOD at 0.443 and 0.665 µm that allow reproducing the measured top of atmosphere reflectances at 0.443 and 0.665 µm using pre-calculated aerosol scattering functions for aerosol models described by a Junge Power-Law size distribution and a constant refractive index of 1.45 – 0.0i. The outputs of the algorithm are the AOD at 0.443 µ m and the aerosol Ångström exponent derived between 0.443 and 0.665 µm.

Cloud contamination is the main issue of the standard product as the MERIS cloud mask is not robust enough over land. Assessing the use of the common cloud mask derived from AATSR APOLLO (together with the safety zone) was thus of high interest for this MERIS algorithm, although this led to a reduction of the available swath width. Furthermore, the common Aerosol_cci aerosol components were implemented together with their geospatial prescription through the common aerosol type climatology (since MERIS has not enough information to retrieve the aerosol mixing fractions).

4.7 The aerosol load and altitude from MERIS over ocean retrieval for MERIS (ALAMO, ocean only)

The MERIS ALAMO (Aerosol Load and Altitude from MERIS over Ocean) algorithm has been primarily developed for aerosol altitude retrievals using MERIS data. Necessary inputs for altitude retrievals, such as aerosol optical properties, are derived in a first step with an initial assumption on the layer altitude. The cloud masking and AOD retrieval schemes are a close adaptation of the MODIS algorithm (Tanré et al., 1997; Remer et al., 2005), using only the following MERIS bands: 0.51, 0.56, 0.665, 0.75375 and 0.865 µm. Due to spectral characteristics of MERIS, ALAMO is limited to a maximum wavelength of 0.865 µm and only two pieces of information on aerosol properties can therefore be retrieved instead of three parameters with MODIS. MERIS aerosols products are retrieved with a spatial resolution of 10 × 10 pixels (12 × 12 km^2). This resolution allows (i) an adequate signal-to-noise ratio (SNR) for a better characterisation of the aerosols type and (ii) rejection of pixels considered as non-valid through statistics criteria, in order to ensure the quality of the aerosol product. The aerosol products of ALAMO include the optical depth and the mixing ratio of fine and coarse

AMTD
6, 2353–2411, 2013

modes. Aerosol models used for ALAMO baseline are the same as the ones used for the most current version of MODIS products. In a second step the altitude of the aerosol layer is estimated using the MERIS O_2A absorption channel and following the algorithm described in Dubuisson et al. (2009). A pixel reclassification is done after the altitude retrieval to remove high thin clouds based on a threshold on altitude and spatial variance of altitude.

The set of common Aerosol_cci components was implemented in ALAMO with a number of fixed mixtures.

4.8 The PARASOL retrieval (ocean only)

In the framework of Aerosol_cci, for PARASOL the aerosol retrieval over ocean is only considered. It is based on a comparison between spectral, directional and/or polarized radiances and LUTs built for a set of aerosol models (lognormal size distribution and refractive index), different aerosol optical depth (AOD) and geometrical conditions using the SOS method including polarization computations (Lenoble et al., 2007). The first step of the algorithm is to perform a cloud screening and then correct for gaseous and possible stratospheric contamination. The inversion scheme (Herman et al., 2005) uses the full measurements in the 0.67 and 0.865 µm channels. After surface contamination correction, the atmospheric total and polarized radiances are calculated according to the approximation of Wang and Gordon (1994). Thanks to the use of directional and polarized information, several parameters (size, refractive index, shape) of the aerosol models can be derived when the scattering angle range is large enough (at least 125°–155°).

The aerosol models used in the baseline version of the PARASOL algorithm include four fine mode, one spherical coarse mode and one non-spherical coarse mode components. For the non-spherical mode, the phase matrix is directly obtained from Volten et al. (2001); the size parameters r_0 and σ_0 are assumed equal to the values of the spherical coarse mode; no values are assigned for the refractive index. The non-spherical fraction within the coarse mode is set to five discrete values: 0.00, 0.25, 0.50, 0.75 and 1.00. When using the Aerosol_cci components in free retrieval the algorithm did not mix the two fine mode aerosol components.

Unlike ENVISAT, the equatorial crossing time of PARASOL is 01:30 p.m., which makes the use of the APOLLO AATSR common cloud mask irrelevant. Thus for PARASOL only the internal cloud detection scheme based on several tests (threshold on NIR and SWIR reflectances, spatial variability of reflectances, detection of the polarized rainbow, corresponding to the presence of water droplets) is used and has been shown efficient (Bréon and Colzy, 1999).

LUT's are computed for a rough ocean surface with a constant wind speed of 5 $m\,s^{-1}$ for considering the ocean-atmosphere interactions. The foam contribution is calculated according to the Koepke's model (1984) with a constant value 0.22 for the foam reflectance. The ocean colour reflectance is taken equal to zero at 0.865 µm and to 0.001 at 0.670 µm. A glint mask is applied based on the computation of the reflectances using the wind speed as an input of the Cox and Munk (1954) model.

5 Results of algorithm experiments

5.1 Evaluation approach

For evaluation $1^{\circ} \times 1^{\circ}$ gridded level 3 satellite datasets produced with the Aerosol_cci experiments covering the month of September 2008 were compared with daily averaged AERONET sun photometer data (daylight hours only). The daily satellite data (in fact one daytime snapshot per satellite) were retrieved on the days when AERONET observations in the grid were reported. Coherent pairs of valid daily observation from satellite and sun photometer were thus retained at each station for clear-sky conditions where both sun photometer and satellite retrievals were successful.

AeroCom tools were used to evaluate the Aerosol_cci satellite retrieval versions. These tools had been developed originally for the evaluation of aerosol models within the AeroCom initiative. To quantify the performance of the different versions of the retrieval algorithms in the experiments, reference data sets were compiled from sun photometer data. Aerosol optical properties of high quality are provided by the ground-based sun-/sky photometer networks of AERONET, PHOTONS, SKYnet and GAW (Holben, 2001). In contrast to aerosol remote sensing from space these ground based transmission measurements require no a-priori assumption of aerosol absorption or radiative background. The error in individual retrieved aerosol optical depth measurements has been estimated (Eck et al., 1999; Dubovik et al., 2002) to be ~ 0.01, or 5–10 % for AOD values smaller than 0.2. Using AERONET reference data averaged over the day somewhat increased their uncertainties in cases of highly variable aerosol conditions. Even though limited to the land based observation sites, having access to a global set of sun-/sky-photometer data provided the possibility to establish solid statistics. In this evaluation total AOD at 0.55 µm from the direct sun observations of AERONET, level 2, version 3 were used.

Scatter plots, histograms, scores, time series, bias visualisation on a map or as a function of latitude summarize overall skill. The graphical display of these comparisons can be publically accessed (e.g. http://aerocom.met.no/cgi-bin/aerocom/surfobs_annualrs.pl?MODELLIST=SATELLITES). Comparisons were made for the globe and regionally e.g. for North Africa, Europe, China, India, North America. This paper focuses on the global analysis.

AeroCom tools also provide monthly mean AOD maps calculated from daily satellite data. These monthly mean maps were also visibly analysed in order to judge the overall differences between algorithms and versions (or their reduction) and in particular to see how far features of the global aerosol distribution could be resolved by the algorithms.

5.2 Experiment analysis results

So far the following experiments were conducted and are described in this paper: (0) baseline datasets produced with the pre-cursor algorithms prior to any changes; (1) the use of a common set of optical aerosol properties with four components, which were externally mixed; (2) the additional use of an AeroCom/AERONET based aerosol

AMTD
6, 2353–2411, 2013

type climatology as a priori information; (3) the use of a common AATSR nadir cloud mask for all ENVISAT algorithms. Table 3 lists the experiments conducted and the numbers used in the following analysis for the different algorithms. Not all algorithms could conduct all experiments due to a number of technical constraints.

As initial way of assessing the results of the various experiments Figs. 6–10 provide maps of monthly mean (simple average of all gridded daily AOD values) for September 2008. These maps allowed to check whether typical large scale features of the global aerosol distribution could be retrieved by the various algorithms (e.g. biomass burning plumes west of Southern Africa, dust plume west of the Sahara, seasonal biomass burning in South America and Southern Africa, industrial/urban pollution in West China and India, low AOD values in remote oceanic regions and higher mid-latitudes and over large mountain regions such as Tibet or the Rocky Mountains, dust loading in semi-arid regions). Also the global coverage of the different datasets could be estimated, showing some differences in extending to high latitudes and cloud-induced gaps in the tropics.

Figure 6 shows the baseline datasets for all eight algorithms prior to the experiments. Clearly, there is qualitative agreement on several of the characteristic features. However, there are also many qualitative and quantitative differences between the maps over land and ocean (e.g. global oceans, biomass burning in South America and Africa, industrial pollution in Eastern China and India, Europe and North America).

Figure 7 shows the results of the first experiment using the common aerosol components for seven of the retrievals. There is a general tendency for better agreement of the features in the maps for most but not all of the algorithms. High AOD regions of biomass burning in South America and Central/South Africa and over adjacent oceans as well as of Northern African dust are now at least partly visible in all of them. Also over India, Eastern China, Europe and North America the differences between most of the datasets are reduced, although still the features do still not agree everywhere. Four algorithms have now similar background oceanic AOD (and the other three agree at

Discussion Paper | Discussion Paper | Discussion Paper | Discussion Paper |

AMTD

6, 2353–2411, 2013

Aerosol retrieval experiments in the ESA Aerosol_cci project

T. Holzer-Popp et al.

least in the tropics). MERIS has very high AOD in high latitudes and for SYNAER the high AOD features in Central Asia of the baseline dataset get even more pronounced.

Figure 8 shows the results of the second experiment for five algorithms, where the AeroCom/AERONET climatology was used as a priori information for the aerosol mixing fractions. Here, the agreement of features over land between the three AATSR and the one MERIS algorithm in the (sub-)tropics is enhanced further. ADV shows very high AOD in high latitudes and increased AOD over tropical oceans. SYNAER has generally much lower AOD, which is assumed to be partly linked to an interplay of aerosol absorption (now prescribed by the climatology) and the surface parameterization developed using different assumptions on aerosol absorption. Over ocean some retrievals seem to completely fail with the climatology-prescribed aerosol mixture (not meeting fit quality criteria).

The use of the common cloud mask in the third experiment is shown for four retrievals in Fig. 9. It is noted that ADV and MERIS-STD used the common climatology (thus comparing experiment 3 directly to experiment 2), while SU and SYNAER went back to free retrieval (thus comparing experiment 3 to experiment 1). The impact of using the common cloud mask is relatively small for the retrievals using AATSR. For SYNAER (where only the size of the safety zone was changed because APOLLO was used in the baseline version already) a reduction of numbers of available dark fields was observed, which led to a minor change of the resulting map. The largest change is visible in the MERIS-STD dataset, when using the AATSR-based common cloud mask with a significant reduction in coverage and a general reduction of AOD values.

For a quantitative analysis Figs. 10 to 13 show the scatter plots of satellite AOD at 0.55 µm versus AERONET (all gridded daily means) for the datasets produced by the various algorithms and experiments as shown in Figs. 6–9. It is obvious that, except for PARASOL, all datasets showed a clearly weaker performance than reference datasets (e.g. MODIS, MISR).

For each algorithm and each experiment conducted the results of the analysis are summarized in Table 4 which shows clearly that the number of data points coincident

AMTD
6, 2353–2411, 2013

with AERONET observations may change significantly between the different algorithms and between the experiments. Evidently, the wider swath of MERIS had to provide larger numbers of data points compared to AATSR. The synergetic retrieval constrained by two instruments and with even larger pixel size had as expected the lowest number of data points. PARASOL also has a large pixel size resulting in fewer data points. But even if the same sensor was used the numbers differed due to different quality thresholds for cloud free super pixels of $10 \times 10\,\mathrm{km}^2$ within the level 2 products. Outstanding changes in numbers of data pairs between experiments of one algorithm are obvious for MERIS. For the MERIS standard algorithm using the common cloud mask based on AATSR led to a major decrease as one would expect due to the reduction to half of the swath width. However, the decrease went much further and yielded even significantly less pixels than for AATSR only algorithms. The reason for this needs further investigation. Interestingly, for ALAMO the coverage almost doubled with using the common aerosol components while SYNAER had a reduced number of data pairs. This indicates sensitivity in algorithm convergence depending on aerosol assumptions.

Interpreting the different inter-comparisons needs some caution due to these different numbers of data pairs since the statistical basis may exhibit important changes (e.g. adding or deleting difficult points). This is, why also the visual assessment of aerosol features and coverage in the monthly mean maps discussed earlier was taken into account. No filter for common data points over all four experiments and eight algorithms has been applied, since it would have reduced the number of common points in all 24 datasets to a statistically weak sample. In the round robin analysis (de Leeuw et al., 2013) such common filtering to ensure that matching data pairs were assessed could be applied to the smaller number of datasets (e.g. three AATSR or three MERIS datasets).

The statistical parameters listed in Table 4 are plotted in Fig. 14 in order to get a better overview of results of the experiments. It should be noted that for two of the eight algorithms only results over ocean are available (circled in the plots), where correlation values are typically higher and rmse lower than over land.

AMTD
6, 2353–2411, 2013

Figure 14 shows following major changes in the sequence of experiments: for AATSR only algorithms the introduction of the common aerosol properties and/or the use of the AeroCom/AERONET climatology as a priori led to a clear improvement of correlations and partly to a slight reduction of rmse and/or bias, whereas the use of the common cloud mask showed little or even a small negative effect. For SYNAER the bias was reduced by the common aerosol properties and even further by the increased safety zone in the cloud mask (probably reducing remaining cloud contamination), but the use of the aerosol type climatology increased the bias, which is probably due to the fact, that the surface parameterization used for all experiments has too bright surface albedo assumptions and thus prefers wrong aerosol absorption. The MERIS algorithms did not benefit from the common aerosol properties with or without a priori aerosol type climatology use. Using the AATSR-based common cloud mask led to a slight improvement of all statistical parameters for the MERIS standard algorithm. For PARASOL a clear positive effect was seen on rmse but a small adverse effect on correlation when introducing the common aerosol components. It should be noted that this analysis of quantitative changes was done on global average.

6 Discussion and conclusions

In Aerosol_cci several experiments were conducted in order to understand the role of major modules in eight European aerosol retrieval algorithms. For the experiments datasets covering the entire globe and one complete month (September 2008) were produced in order to allow significant statistical analysis and include cases in all climate zones and with all major types of aerosol. It can be questioned, whether a one month global dataset is sufficient for identifying the impacts of algorithms changes, but it was chosen as a pragmatic trade-off between statistical soundness and processing efforts. The subsequent analysis steps (round robin exercise with 4 months, one in each season, see de Leeuw et al. (2013) and validation with complete 12 months of the same year, not yet published) proof that the limited analysis of only one month of global data

AMTD
6, 2353–2411, 2013

summarized here has helped to identify possible improvements (both, demonstrated in this paper such as the revised optical aerosol model, and identified for subsequent algorithm development such as post-processing to reduce cloud contamination) and to ultimately reach algorithms which performed significantly better than the baseline algorithms.

The evaluation of the datasets was conducted by assessing statistical parameters (mean bias, root mean square error – rmse, and Pearson correlation coefficient) of gridded 1° latitude longitude daily satellite products (level 3) versus AERONET daily averaged aerosol optical depth (AOD) interpolated to a reference wavelength at 0.55 µm for all retrievals and the sun photometer measurements. All experiments started from an analysis of baseline datasets for each algorithm prior to any changes. Up to three experiments were conducted for the various pre-cursor algorithms: use of common optical aerosol properties, use of a common aerosol type climatology, use of common cloud mask.

Across algorithms the use of a common definition of aerosol components harmonized the retrievals (in terms of their internal construction), but it did not harmonize their results (i.e. their results do not obviously converge; see Fig. 14). However, it led to improvement of all algorithms (except two for MERIS) in at least one or sometimes several statistical parameters (including coverage). Additionally using a common climatology of aerosol type led to an additional improvement for several algorithms, but could also reduce the algorithm performance. Using the common cloud mask (which still had important deficiencies, namely missing forward cloud mask, missing dust flag), led to minor changes or even decreased accuracy for one algorithm. On the other hand, an increased size of the safety zone around clouds was shown to be beneficial (tested with one algorithm). In the one case of applying the AATSR-based common cloud mask to a MERIS algorithm a clear improvement in all statistical parameters was shown, but at the cost of a major reduction in pixel numbers. In general, data filtering needs further assessment to achieve the optimal trade-off between highest possible coverage and capability to cover regional (and seasonal) features versus highest accuracy, since an

AMTD
6, 2353–2411, 2013

anti-correlation between number of data and accuracy is indicated in the results shown in Table 4.

The experiments allowed studying the sensitivities of each participating algorithm and drawing conclusions for the improved setup of the round robin algorithm in the subsequent analysis step. For all three AATSR algorithms the common definition of aerosol components should be used, whereas a priori constraints on the mixing ratios from the climatology should only be used for ADV and for SU over land. Over ocean SU coverage was reduced significantly by using the climatology and for ORAC overall accuracy decreased slightly. The common cloud mask which could only be tested for ADV and SU algorithms should not be used in the form tested in the third experiment (without forward mask and dust flag) since it had little impact (ADV) or even decreased accuracy (SU) and introduces an additional external dependence. In the ORAC algorithm an error occurred in the common cloud mask implementation which needs correction. In general for AATSR algorithms further work was identified as necessary for reducing cloud contamination by post-processing. Additionally, problems in high latitudes were found for ADV which need analysis and correction. Among the three AATSR algorithms SU seems to be more accurate overall which might be due to the advanced surface treatment, but the good results might also be due to the stricter quality control, which results in relatively poor coverage. It is pointed out, that the purpose of this study was not to select a "best" algorithm among those for one sensor – this task is part of the subsequent round robin exercise.

For SYNAER the common aerosol components and the increased cloud safety zone showed positive impact, but the use of the aerosol type climatology decreased coverage and accuracy. Improving the surface parameterization was identified as highest priority (singular experiment not shown here), before being able to draw further conclusions on the added value of the aerosol type climatology. For all three MERIS algorithms the common aerosol components should be used for consistency with the AATSR results although for the algorithm versions tested this led to some reduction in product accuracy. In particular for the ALAMO algorithm over ocean the common

AMTD
6, 2353–2411, 2013

components should be used, since they increased coverage significantly with only a limited reduction in accuracy. Since cloud mask (only tested for the ESA operational algorithm) allowed to improve the accuracy, but at the cost of a significantly reduced coverage, a user-oriented trade-off between coverage and accuracy with regard to the cloud contamination is needed for each application. For the PARASOL algorithm the stability of its results with regard to the assumptions on aerosol properties was proven together with a reduced noise when using the common components.

So far the highest accuracy was observed for PARASOL (ocean only) with really convincing numbers. The three AATSR retrievals showed clear improvement over the various experiments. The nadir only algorithms (MERIS, SYNAER) which are more dependant in all experiments on their surface parameterizations need further improvement; MERIS algorithms also are very sensitive to cloud contamination with the opportunity for improvement in synergy with AATSR.

In conclusion it can be stated, that the experiments revealed opportunities for algorithm improvement (before all the common aerosol components and partly also the a priori aerosol mixing climatology) and identified critical sensitivities where further work is needed. For cloud masking improvement was achieved for MERIS by using the AATSR mask derived with also thermal bands (but only with significant reduction of coverage). Generally, other means of reducing remaining cloud contamination such as larger safety zone (tested for SYNAER) or post-processing (tested in ADV, de Leeuw et al., 2013) seem to have higher potential for improvement, but may lead to overlooking significant aerosol loading near clouds. It should be noted, that the cloud screening in AERONET leads to a bias to cloud-free conditions, so that evaluation of different cloud masks is limited in its extent.

To some extent harmonization between different algorithms also using different sensors and principles has been achieved by the use of common optical aerosol components and an aerosol mixing a priori climatology. This is important as it will facilitate future merged datasets, now that AOD of each component can be really compared between the retrievals. Technically, also the harmonization of the cloud mask for morning

AMTD
6, 2353–2411, 2013

retrievals using AATSR results also for MERIS and SCIAMACHY, has been achieved. However, the common cloud mask itself needs further improvement: processing of forward cloud masks, improving the dust flag to discriminate desert dust outbreaks from clouds. Additionally, the post-processing applied as secondary means to avoid cloud contamination and for quality filtering need also harmonization to assure best matching comparisons.

In a subsequent step of Aerosol_cci the analysis has been extended from one month of global data to four months (one in each season) to further substantiate the results with a larger data amount in a round robin analysis (de Leeuw et al., 2013) but then limited to only one "best" version for each algorithm. The choices for these "best" algorithm versions in this round robin exercise have been based on the experiments described in this paper. This subsequent step showed further, partly significant improvements of several of the algorithms assessed in this paper by improving further elements (e.g. post-processing to avoid cloud contamination) and by detecting and correcting bugs in some algorithms. Ultimately a full global one year dataset of Aerosol Essential Climate Variables will be produced and will be validated and assessed by aerosol climate model users.

As one potentially critical element of aerosol retrievals, the treatment of brightness and directional reflections of land surfaces could not be assessed by similar experiments since it is in parts a core component of each algorithm that cannot be easily modified. Furthermore, it has different importance for different classes of algorithms: dual or multiple viewing instruments (AATSR, PARASOL, MISR) avoid to a first order any dependence on surface brightness by constraining the directional ratios of surface reflectances between various wavelengths or by fully retrieving surface directional behaviour. Nadir only algorithms (MERIS, synergetic AATSR+SCIAMACHY), on the other hand, are dependent on an assumption or parameterization (from vegetation index and mid-infrared reflectances) of surface brightness (of dark fields or all pixels). It is thus planned to use atmospherically corrected MODIS reflectance data around selected

AMTD
6, 2353–2411, 2013

AERONET stations in order to assess the parameterizations used in the respective precursor algorithms.

Over ocean it can generally be assumed that the surface reflectance is very low in red and infrared bands. However, for specific situations (wind speed dependant white cap fraction, coastal sediments and chlorophyll) this assumption is not valid and auxiliary datasets and parameterizations need to be used. Here, preparations have been made to harmonize auxiliary data (e.g. ECMWF re-mapped wind field analysis) where this is feasible. However, for sediments and chlorophyll, the use of an external climatology or daily dataset would mean that the aerosol-surface separation has already been solved in a different retrieval. Furthermore, evaluation of AOD and surface treatment over ocean is difficult due to low numbers of ground-based (ship) observations – at least for September 2008 no significant dataset was available.

The results of all analysis steps are available at the Aerosol_cci project website http://www.esa-aerosol-cci.org, where all datasets, experiments and documents are published to the scientific community; from there also links to the ftp data server at ICARE (accessible on request) and the open AeroCom and ICARE visualization and analysis tools are provided.

Acknowledgement. The results presented in this paper were achieved within the ESA Aerosol_cci project. We acknowledge also AERONET sun photometer data providers through which ground based measurements for the evaluation activities in the project were acquired. Furthermore we acknowledge the supporting teams at AeroCom, ICARE and WDC-RSAT (hosted by DLR) which played a crucial role in the data evaluation, data storage services and documentation.

The service charges for this open access publication have been covered by a Research Centre of the Helmholtz Association.

AMTD

6, 2353–2411, 2013

References

Bevan, S. L., North, P. R. J., Grey, W. M. F., Los, S. O., and Plummer, S. E.: Impact of atmospheric aerosol from biomass burning on Amazon dry-season drought, J. Geophys. Res., 114, D09204, doi:10.1029/2008JD011112, 2009.

Bevan, S. L., North, P. R. J., Los, S. O., and Grey, W. M. F.: A global dataset of atmospheric aerosol optical depth and surface reflectance from AATSR, Remote Sens. Environ., 116, 119–210, 2012.

Bréon, F. M. and Colzy, S.: Cloud detection from the spaceborne POLDER instrument and validation against surface synoptic observations, J. Appl. Meteorol., 38, 777–785, 1999.

Coakley, J. A., Friedman, M. A., and Tahnk, W. R.: Retrieval of cloud properties for partly cloudy imager pixels, J. Atmos. Ocean. Tech., 22, 3–17, doi:10.1175/JTECH-1681.1, 2005.

Cox, C. and Munk, W.: Measurements of the roughness of the sea surface from photographs of the Sun's glitter, J. Opt. Soc. Amer., 44, 838–850, 1954.

Curier, L., de Leeuw, G., Kolmonen, P., Sundström, A.-M., Sogacheva, L., and Bennouna, Y.: Aerosol retrieval over land using the (A) ATSR dual-view algorithm, in: Satellite Aerosol Remote Sensing Over Land, edited by: Kokhanovsky, A. A. and de Leeuw, G., Springer, Berlin, 135–160, 2009.

De Leeuw, G., Holzer-Popp, T., Bevan, S., Davies, W., Descloitres, J., Grainger, R. G., Griesfeller, J., Heckel, A., Kinne, S., Klüser, L., Kolmonen, P., Litvinov, P., Martynenko, D., North, P., Ovigneur, B., Pascal, N., Poulsen, C., Ramon, D., Schulz, M., Siddans, R., Sogacheva, L., Tanré, D., Thomas, G. E., Virtanen, T. H., von Hoyningen Huene, W., Vountas, M., and Pinnock, S.: Evaluation of seven European aerosol optical depth retrieval algorithms for climate analysis, Remote Sens. Environ., accepted, 2013.

Dubuisson, P., Frouin, R., Dessailly, D., Duforêt, L., Léon, J.-F., Voss, K., and Antoine, D.: Estimation of aerosol altitude from reflectance ratio measurements in the O2 A-band, Remote Sens. Environ., 113, 1899–1911, 2009.

Dubovik, O. and King, M. D.: A flexible inversion algorithm for retrieval of aerosol optical properties from Sun and sky radiance measurements, J. Geophys. Res., 105, 20673–20696, 2000.

Dubovik, O., Holben, B., Eck, T. F., Smirnov, A., Kaufman, Y. J., King, M. D., Tanré, D., and Slutsker, I.: Variability of absorption and optical properties of key aerosol types observed in worldwide locations, J. Atmos. Sci., 59, 590–608, 2002.

AMTD
6, 2353–2411, 2013

Dubovik, O., Sinyuk, A., Lapyonok, T., Holben, B. N., Mishchenko, M., Yang, P., Eck, T. F., Volten, H., Munoz, O., Veihelmann, B., van der Zander, W. J., Sorokin, M., and Slutsker, I.: Application of spheroid models to account for aerosol particle nonsphericity in remote sensing of desert dust, J. Geophys. Res., 111, D11208, doi:10.1029/2005JD006619, 2006.

Eck T. F., Holben, B. N., Reid, J. S., Dubovik, O., Kinne, S., Smirnov, A., O'Neill, N. T., and Slutsker, I.: The wavelength dependence of the optical depth of biomass burning, urban and desert dust aerosols, J. Geophys. Res., 104, 31333–31350, 1999.

Flowerdew, R. J. and Haigh, J. D.: An approximation to improve accuracy in the derivation of surface reflectances from multi-look satellite radiometers, Geophys. Res. Lett., 22, 1693–1696, 1995.

Grey, W. M. F., North., P. R. J., Los, S. O., and Mitchell, R. M.: Aerosol optical depth and land surface reflectance from multi-angle AATSR measurements: global validation and intersensor comparisons, IEEE T. Geosci. Remote, 44, 2184–2197, 2006a.

Grey, W. M. F., North, P. R. J., and Los, S. O.: Computationally efficient method for retrieving aerosol optical depth from ATSR-2 and AATSR data, Appl. Optics, 45, 2786–2795, 2006b.

Herman, M., Deuzé, J. L., Marchand, A., Roger, B., and Lallart, P.: Aerosol remote sensing from POLDER/ADEOS over the ocean: Improved retrieval using a nonspherical particle model, J. Geophys. Res., 110, D10S02, doi:10.1029/2004JD004798, 2005.

Hess, M., Köpke, P., and Schult, I.: Optical properties of aerosols and clouds: the software package OPAC, B. Am. Meteorl. Soc., 79, 831–844, 1998.

Holben, B. N., Eck, T. F., Slutsker, I., Tanre, D., Buis, J. P., Setzer, A., Vermote, E., Reagan, J. A., Kaufman, Y. J., Nakajima, T., Lavenu, F., Jankowiak, I., and Smirnov, A.: AERONET – a federated instrument network and data archive for aerosol characterization, Remote Sens. Environ., 66, 1–16, 1998.

Holben, B. N., Tanre, D., Smirnov, A., Eck, T. F., Slutsker, I., Abuhassan, N., Newcomb, W. W., Schafer, J., Chatenet, B., Lavenue, F., Kaufman, Y. J., Castle, J. V., Setzer, A., Markham, B., Clark, D., Frouin, R., Halthore, R., Karnieli, A., O'Neill, N. T., Pietras, C., Pinker, R. T., Voss, K., and Zibordi, G.: An emerging ground-based aerosol climatology: aerosol optical depth from AERONET, Geophys. Res., 106, 12067–12097, 2001.

Hollmann, R., Merchant, C., Saunders, R., Downy, C., Buchwitz, M., Cazenave, A., Chuvieco, E., Defourny, P., de Leeuw, G., Forsberg, R., Holzer-Popp, T., Paul, F., Sandven, S., Sathyendranath, S., van Roozendael, M., and Wagner, W.: The ESA climate change initia-

AMTD
6, 2353–2411, 2013
Aerosol retrieval experiments in the ESA Aerosol_cci project
T. Holzer-Popp et al.

tive: satellite data records for essential climate variables, B. Am. Meteorol. Soc., in review, 2013.
Holzer-Popp, T., Schroedter, M., and Gesell, G.: Retrieving aerosol optical depth and type in the boundary layer over land and ocean from simultaneous GOME spectrometer and ATSR-2 radiometer measurements, 1. Method description, J. Geophys. Res., 107, 4578, doi:10.1029/2001JD002013, 2002.
Holzer-Popp, T., Schroedter-Homscheidt, M., Breitkreuz, H., Martynenko, D., and Klüser, L.: Improvements of synergetic aerosol retrieval for ENVISAT, Atmos. Chem. Phys., 8, 7651–7672, doi:10.5194/acp-8-7651-2008, 2008.
IPCC: Solomon, S., Qin, D., Manning, M., Chen, Z., Marquis, M., Averyt, K. B., Tignor, M., and Miller, H. L. (Eds.): Climate Change: The Physical Science Basis, Contribution of Working Group I to the Fourth Assessment Report of the Intergovernmental Panel on Climate 490 Change (IPCC), Cambridge University Press, Cambridge (UK), New York (USA), 996 pp., 2007.
Kinne, S., Schulz, M., Textor, C., Guibert, S., Balkanski, Y., Bauer, S. E., Berntsen, T., Berglen, T. F., Boucher, O., Chin, M., Collins, W., Dentener, F., Diehl, T., Easter, R., Feichter, J., Fillmore, D., Ghan, S., Ginoux, P., Gong, S., Grini, A., Hendricks, J., Herzog, M., Horowitz, L., Isaksen, I., Iversen, T., Kirkevåg, A., Kloster, S., Koch, D., Kristjansson, J. E., Krol, M., Lauer, A., Lamarque, J. F., Lesins, G., Liu, X., Lohmann, U., Montanaro, V., Myhre, G., Penner, J., Pitari, G., Reddy, S., Seland, O., Stier, P., Takemura, T., and Tie, X.: An AeroCom initial assessment – optical properties in aerosol component modules of global models, Atmos. Chem. Phys., 6, 1815–1834, doi:10.5194/acp-6-1815-2006, 2006.
Koepke, P.: Effective reflectance of the oceanic whitecaps, Appl. Optics, 23, 1816–1824, 1984.
Kokhanovsky, A. A. and de Leeuw, G.: Satellite Aerosol Remote Sensing Over Land, Springer, Berlin, 135–160, 2009.
Kolmonen, P., Sundström, A.-M., Sogacheva, L., Rodriguez, E., Virtanen, T. H., and de Leeuw, G.: The uncertainty characterization of AOD for the AATSR ADV/ASV retrieval algorithm – towards the assimilation of the satellite retrieved aerosol properties, Atmos. Meas. Tech. Discuss., in review, 2013.
Koren, I., Remer, L. A., Kaufman, Y. J., Rudich, Y., and Vanderlei-Martins, J.: On the twilight zone between clouds and aerosols, Geophys. Res. Lett., 34, L08805, doi:10.1029/2007GL029253, 2007.

AMTD
6, 2353–2411, 2013

Koren, I., Oreopoulos, L., Feingold, G., Remer, L. A., and Altaratz, O.: How small is a small cloud?, Atmos. Chem. Phys., 8, 3855–3864, doi:10.5194/acp-8-3855-2008, 2008.
Kriebel, K. T., Gesell, G., Kästner, M., and Mannstein, H.: The cloud analysis tool APOLLO: improvements and validations, Int. J. Remote Sens., 24, 2389–2408, 2003.
Lenoble, J., Herman, M., Deuzé, J. L., Lafrance, B., Santer, R., and Tanré, D.: A successive order of scattering code for solving the vector equation of transfer in the Earth's atmosphere with aerosols, J. Quant. Spectrosc. Ra., 107, 479–507, 2007.
Maignan, F., Bréon, F.-M., and Lacaze, R.: Bidirectional reflectance of Earth targets: evaluation of analytical models using a large set of spaceborne measurements with emphasis on the hot spot, Remote Sens. Environ., 90, 210–220, 2004.
Nagel, M. R., Quenzel, H., Kweta, W., and Wendling, P.: Daylight Illumination-Color-Contrast-Tables, New York, Academic Press, 1978.
North, P. R. J.: Estimation of aerosol opacity and land surface bidirectional reflectance from ATSR-2 dual-angle imagery: operational method and validation, J. Geophys. Res., 107, 1–11, doi:10.1029/2000JD000207, 2002.
North, P. R. J., Briggs, S. A., Plummer, S. E., and Settle, J. J.: Retrieval of land surface bidirectional reflectance and aerosol opacity from ATSR-2 multi-angle imagery, IEEE T. Geosci. Remote, 37, 526–537, 1999.
Popp, Th.: Correcting atmospheric masking to retrieve the spectral albedo of land surfaces from satellite, Int. J. Remote Sens., 16, 3483–3508, 1995.
Poulsen, C. A., Siddans, R., Thomas, G. E., Sayer, A. M., Grainger, R. G., Campmany, E., Dean, S. M., Arnold, C., and Watts, P. D.: Cloud retrievals from satellite data using optimal estimation: evaluation and application to ATSR, Atmos. Meas. Tech., 5, 1889–1910, doi:10.5194/amt-5-1889-2012, 2012.
Ramon, D. and Santer, R.: Operational remote sensing of aerosols over land to account for directional effects, Appl. Optics, 40, 3060–3075, 2001.
Rodgers, C. D.: Inverse Methods for Atmospheric Sounding: Theory and Practice, World Scientific, Singapore, 2000.
Remer, L. A., Kaufman, Y. J., Tanré, D., Mattoo, S., Chu, D. A., Martins, J. V., Li, R. R., Ichoku, C., Levy, R. C., Kleidman, R. G., Eck, T. F., Vermote, E., and Holben, B. N.: The MODIS aerosol algorithm, products, and validation, J. Atmos. Sci., 62, 947–973, 2005.
Santer, R., Carrere, V., Dubuisson, P., and Roger, J. C.: Atmospheric correction over land for MERIS, Int. J. Remote Sens., 20, 1819–1840, 1999.

Santer, R., Ramon, D., Vidot, J., and Dilligeard, E.: A surface reflectance model for aerosol remote sensing over land, Int. J. Remote Sens., 28, 737–760, 2007.
Saunders, R. W. and Kriebel, K. T.: An improved method for detecting clear sky and cloudy radiances from AVHRR data, Int. J. Remote Sensing, 9, 123–150, 1988.
Sayer, A. M., Thomas, G. E., and Grainger, R. G.: A sea surface reflectance model for (A)ATSR, and application to aerosol retrievals, Atmos. Meas. Tech., 3, 813–838, doi:10.5194/amt-3-813-2010, 2010.
Sayer, A. M., Poulsen, C. A., Arnold, C., Campmany, E., Dean, S., Ewen, G. B. L., Grainger, R. G., Lawrence, B. N., Siddans, R., Thomas, G. E., and Watts, P. D.: Global retrieval of ATSR cloud parameters and evaluation (GRAPE): dataset assessment, Atmos. Chem. Phys., 11, 3913–3936, doi:10.5194/acp-11-3913-2011, 2011.
Sayer, A. M., Smirnov, A., Hsu, C., and Holben, B. N.: A pure marine aerosol model, for use in remote sensing applications, J. Geophys. Res., 117, D05213, doi:10.1029/2011JD016689, 2012a.
Sayer, A. M., Thomas, G. E., Grainger, R. G., Carboni, E., Poulsen, C. A., and Siddans, R.: Use of MODIS-derived surface reflectance data in the ORAC-AATSR aerosol retrieval algorithm: impact of differences between sensor spectral response functions, Remote Sens. Environ., 116, 177–188, 2012b.
Seinfeld, J. H. and Pandis, S. N.: Atmospheric Chemistry and Physics: From Air Pollution to Climate Change, Wiley & Sons, New York, ISBN 0-471-17815-2, 1998.
Sinyuk, A., Torres, O., and Dubovik, O.: Combined use of satellite and surface observations to infer the imaginary part of refractive index of Saharan dust, Geophys. Res. Lett., 30, 1081, doi:10.1029/2002GL016189, 2003.
Sinyuk, A., Dubovik, O., Holben, B. N., Eck, T. F., Breon, F.-M., Martonchik, J., Kahn, R., Diner, D. J., Vermote, E. F., Roger, J.-C., Lapyonok, T., and Slutser, I.: Simultaneous retrieval of aerosol and surface properties from a combination of AERONET and satellite data, Remote Sens. Environ., 107, doi:10.1016/j.rse.2006.07.022, 90–108, 2007.
Smith, D.: Report for ATSR VisMon contract, ESA Technical note, Rutherford Appleton Laboratory, Harwell (UK), 2005.
Stamnes, K., Tsay, S. C., and Wiscombe, W.: Numerically stable algorithm for discrete-ordinate-method radiative transfer in multiple scattering and emitting layered media, Appl. Optics, 12, 2502–2509, 1988.

Tanré, D., Kaufman, Y. J., Herman, M., and Mattoo, S.: Remote sensing of aerosol properties over oceans using the MODIS/EOS spectral radiances, J. Geophys. Res., 102, 16971–16988, 1997.
Thomas, G. E., Carboni, E., Sayer, A. M., Poulsen, C. A., Siddans, R., and Grainger, R. G.: Oxford-RAL Aerosol and Cloud (ORAC): aerosol retrievals from satellite radiometers, in: Aerosol Remote Sensing Over Land, edited by: Kokhanovsky, A. A. and de Leeuw, G., Springer, Berlin, 2009.
Thomas, G. E., Poulsen, C. A., Siddans, R., Sayer, A. M., Carboni, E., Marsh, S. H., Dean, S. M., Grainger, R. G., and Lawrence, B. N.: Validation of the GRAPE single view aerosol retrieval for ATSR-2 and insights into the long term global AOD trend over the ocean, Atmos. Chem. Phys., 10, 4849–4866, doi:10.5194/acp-10-4849-2010, 2010.
Veefkind, J. P. and de Leeuw, G.: A new algorithm to determine the spectral aerosol optical depth from satellite radiometer measurements, J. Aerosol Sci., 29, 1237–1248, 1998.
Vermote, E. F., Tanre, D., Deuze, J. L., Herman, M., and Morcrette, J. J.: Second simulation of the satellite signal in the solar spectrum, 6S: an overview, IEEE T. Geosci. Remote, 35, 675–686, 1997.
Volten, H., Munoz, O., Rol, E., de Haan, J. F., Vassen, W., and Hovenier, J. W.: Scattering matrices of mineral aerosol particles at 441.6 nm and 632.8 nm, J. Geophys. Res., 106, 17375–17401, 2001.
von Hoyningen-Huene, W., Freitag, M., and Burrows, J. P.: Retrieval of aerosol optical thickness over land surfaces from top-of-atmosphere radiances, J. Geophys. Res., 108, 4260, doi:10.1029/2001JD002018, 2003.
von Hoyningen-Huene, W., Kokhanovsky, A., Burrows, J. P., Bruniquel-Pinel, V., and Regner, P.: Simultaneous determination of aerosol- and surface characteristics from top-of-atmosphere reflectance using MERIS on board of ENVISAT, J. Adv. Space Res., 37, 2172–2177, 2006.
Wang, M. and Gordon, H. R.: Radiance reflected from the ocean-atmosphere system: synthesis from individual components of the aerosols size distribution, Appl. Optics, 33, 7088–7095, 1994.
World Meteorological Organization: Implementation plan for the Global Observing System for climate in support of the UNFCCC, GCOS-92, WMO/TD No. 1219, 2004.

AMTD
6, 2353–2411, 2013

Table 1. Log-normal parameters for two coarse and two fine mode aerosol components and their associated mid-visible refractive indices (note, mode number radius and standard deviation [or variance] define the effective radius, which is the 3rd moment to 2nd moment radius ratio). ϖ_0 denotes the single scattering albedo (from de Leeuw et al., 2012).

Aerosol component	Refractive index, real part (0.55 µm)	Refractive index, imaginary part (0.55 µm)	r_{eff} (µm)	Geometric standard deviation (σ_i)	Variance ($\ln \sigma_i$)	Mode radius (µm)	Comments	Aerosol layer height
Dust	1.56	0.0018	1.94	1.822	0.6	0.788	Non-spherical	2–4 km
Sea salt	1.4	0	1.94	1.822	0.6	0.788	AOD threshold constraint	0–1 km
Fine mode weakly absorbing	1.4	0.003	0.140	1.7	0.53	0.07	(ϖ_0 at 0.55 µm: 0.98)	0–2 km
Fine mode strongly absorbing	1.5	0.040	0.140	1.7	0.53	0.07	(ϖ_0 at 0.55 µm: 0.802)	0–2 km

AMTD
6, 2353–2411, 2013

Table 2. Pre-cursor algorithms and sensors targeted in Aerosol_cci total column experiments.

Sensor	Algorithm							
	FMI dual view	ORAC	Swansea dual view	SYNAER	BAER	ESA standard	ALAMO	LOA
Principle	Dual view (land), single view (ocean) Spectral	Dual view Spectral Optimal inter-polation	Dual view Spectral	Nadir Spectral Synergetic dark field/ spectral fit	Nadir spectral	Nadir spectral	Nadir spectral	Multi view Spectral Polarized
							Ocean only	Ocean only
AATSR	×	×	×	×				
MERIS					×	×	×	
SCIAMACHY				×				
PARASOL								×

AMTD
6, 2353–2411, 2013
Aerosol retrieval experiments in the ESA Aerosol_cci project
T. Holzer-Popp et al.

Table 3. Overview of algorithm experiments conducted in Aerosol_cci.

Experiment number	Algorithm experiment definition
0	Baseline (pre-cursor algorithms at start of the proejct)
1	Common optical components (partly) free retrieval
2	Common optical components climatology as a priori aerosol type
3	Common optical components (partly) free retrieval common nadir cloud mask and safety zone

AMTD
6, 2353–2411, 2013

AMTD
6, 2353–2411, 2013

Table 4. Summary of statistical parameters versus AERONET daily mean AOD550 for the experiments conducted. Each cell provides number of data points (N), mean bias (b), rmse (σ) and correlation (R).

		Algorithms							
	Sensors	AATSR			AATSR/ SCIAMACHY	MERIS			PARASOL
Experiment		ADV	ORAC	SU	SYNAER	BAER	Standard	ALAMO only ocean	PARASOL only ocean
0: Baseline	N	456	483	272	228	1078	762	225	420
	b	+0.07	+0.03	−0.02	−0.10	−0.10	+0.04	0.00	+0.03
	Σ	0.26	0.19	0.11	0.18	0.19	0.14	0.13	0.13
	R	0.42	0.53	0.60	0.52	0.21	0.68	0.71	0.85
1: Use of common aerosol model		476	356	374	175	1146		419	373
		+0.01	0.00	−0.03	−0.06	+0.08		+0.05	+0.03
		0.22	0.16	0.13	0.21	0.27		0.18	0.09
		0.42	0.66	0.71	0.55	0.26		0.60	0.83
2: Use of a priori aerosol composition from climatology		432	356	319	217		622		
		+0.02	−0.02	−0.05	−0.13		+0.08		
		0.22	0.16	0.12	0.18		0.17		
		0.56	0.64	0.81	0.50		0.60		
3: Use of common nadir cloud mask		432		311	152		195		
		+0.02		−0.04	−0.01		0.00		
		0.22		0.13	0.19		0.13		
		0.56		0.73	0.51		0.72		

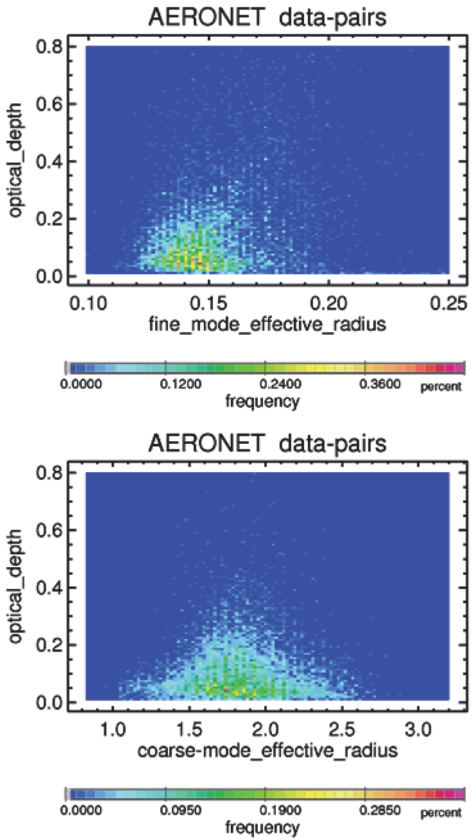

Fig. 1. AERONET probability distribution statistics: The upper image shows the frequency for aerosol sizes smaller than 0.5 µm as function of the associated effective radius (x-axis) and the aerosol optical depth at 0.44 µm (y-axis). The lower image shows the frequency for aerosol sizes larger than 0.5 µm as function of the effective radius (x-axis) and the aerosol optical depth at 0.44 µm (y-axis).

AMTD
6, 2353–2411, 2013

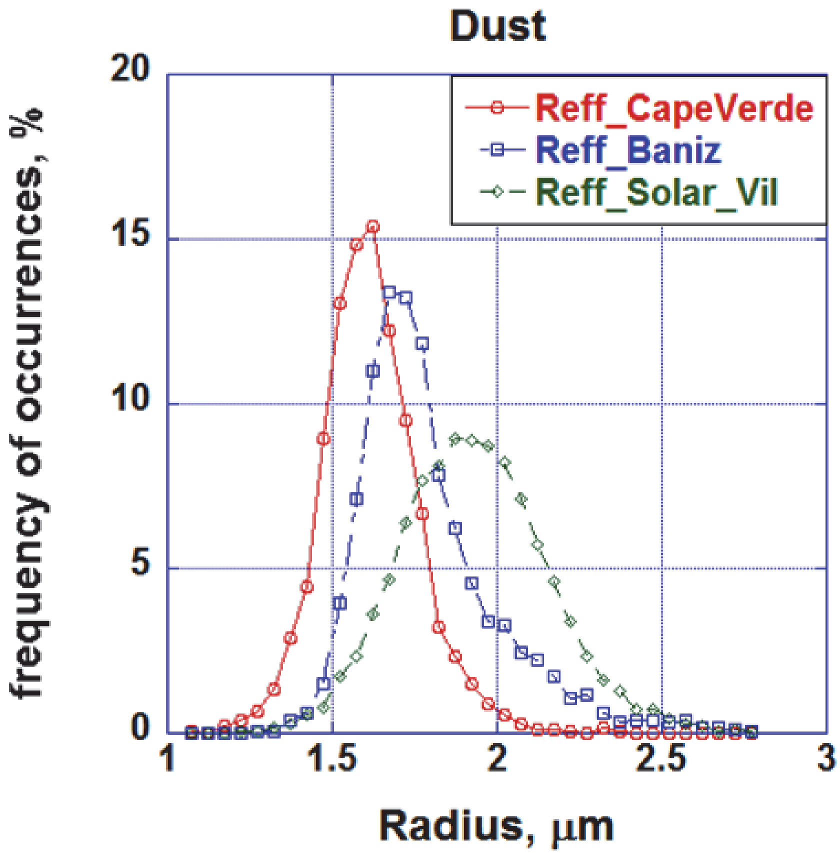

Fig. 2. Dust effective radii distributions for three different AERONET sites Cape Verde, Banizoumbou, and Solar Village.

AMTD
6, 2353–2411, 2013

Title Page
Abstract | Introduction
Conclusions | References
Tables | Figures
◂◂ | ▸▸
◂ | ▸
Back | Close
Full Screen / Esc
Printer-friendly Version
Interactive Discussion

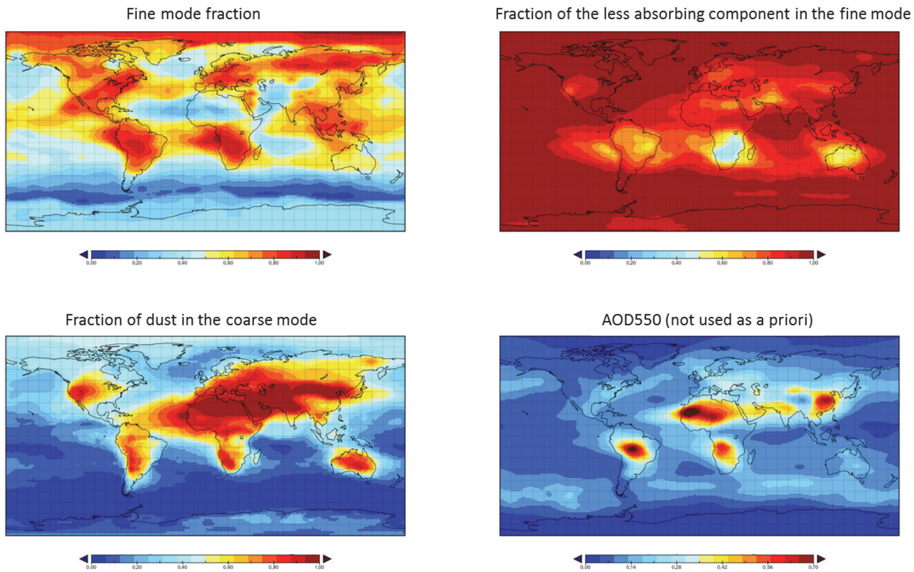

Fig. 3. Climatologies of the three external mixing fractions for the aerosol components of Table 1. The monthly maps shown here are based on AeroCom model median/AERONET AOD550 aerosol type for September; these fractions are used as a priori information for the aerosol type in the retrievals in the second experiment: fine mode fraction (upper left), fraction of less absorbing component in the fine mode (upper right), and fraction of dust in the coarse mode (lower left). As reference (not used as a priori) the AOD550 distribution is also shown (lower right).

AMTD
6, 2353–2411, 2013

Aerosol retrieval experiments in the ESA Aerosol_cci project

T. Holzer-Popp et al.

Title Page
Abstract | Introduction
Conclusions | References
Tables | Figures
◀| |▶
◀ ▶
Back | Close
Full Screen / Esc
Printer-friendly Version
Interactive Discussion

AMTD
6, 2353–2411, 2013

Aerosol retrieval experiments in the ESA Aerosol_cci project

T. Holzer-Popp et al.

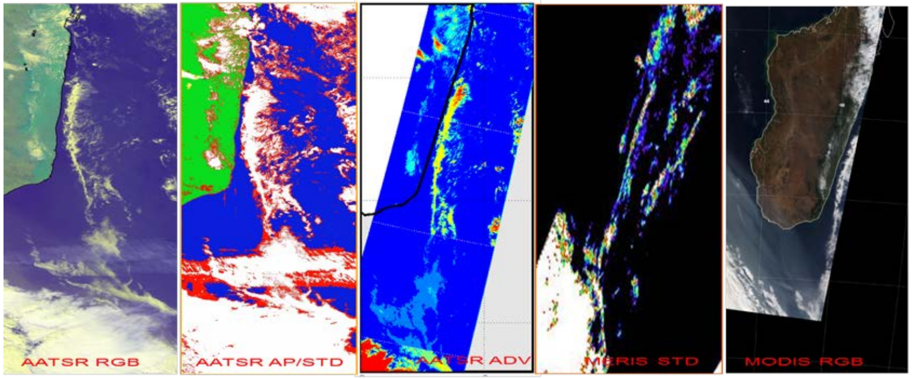

Fig. 4. Single scene analysis example for 1 September 2008 west off Madagascar. From left to right the image shows: AATSR RGB composite, AATSR cloud mask composite from APOLLO and ESA standard masks, AATSR ADV cloud mask, MERIS ESA standard cloud mask, MODIS-Terra true colour RGB composite. The colour codes in the three cloud masks are as follows: AATSR AP/STD: green = land flagged as cloud free in both masks, blue = water flagged as cloud free in both masks, white = both masks agree to flag as cloudy, red = only standard mask flags as cloudy, yellow = only APOLLO flags as cloudy; AATSR ADV: number of positive cloud tests from 0 (dark blue) over green, yellow to red; MERIS STD: cloud fraction from 0 (black) to 1 (white).

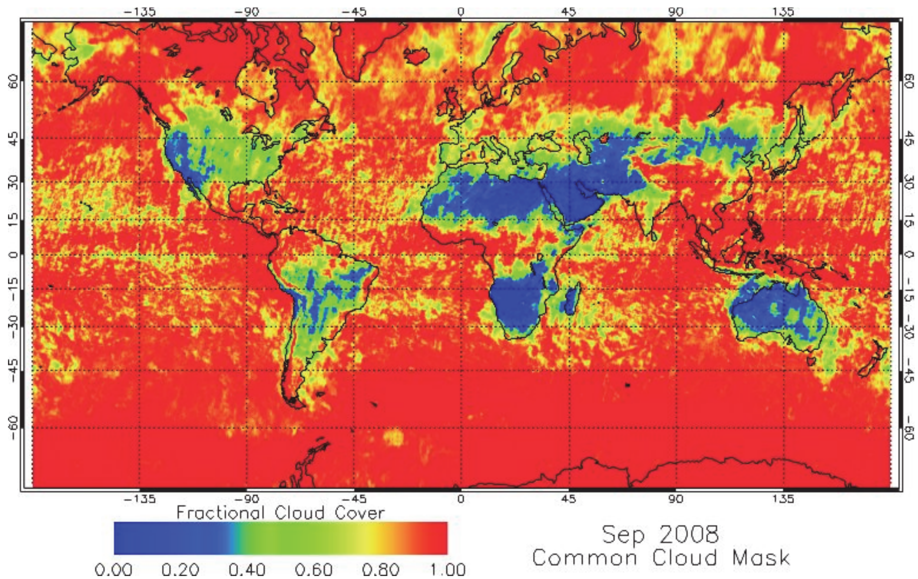

Fig. 5. Global monthly mean cloud cover from DLR APOLLO AATSR (common nadir cloud mask used in Aerosol_cci) for September 2008.

AMTD
6, 2353–2411, 2013

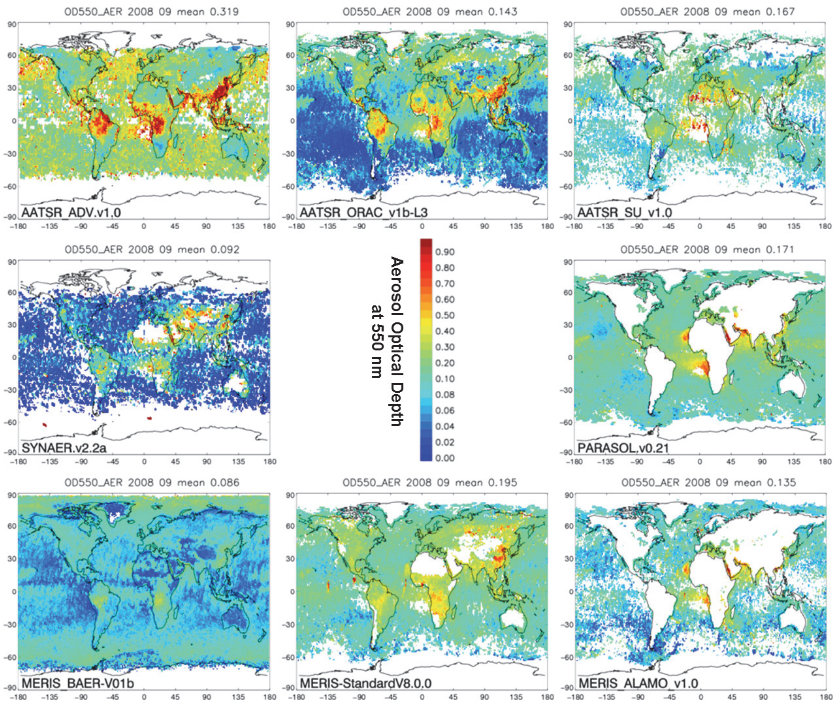

Fig. 6. September 2008 unweighted monthly mean ADO550 for eight total column precursor algorithms: baseline datasets (experiment number 0 in Table 3). From top left to bottom right: AATSR ADV, AATSR ORAC, AATSR SU, SYNAER, MERIS BAER, MERIS STANDARD, MERIS ALAMO (ocean only), PARASOL (ocean only).

AMTD
6, 2353–2411, 2013

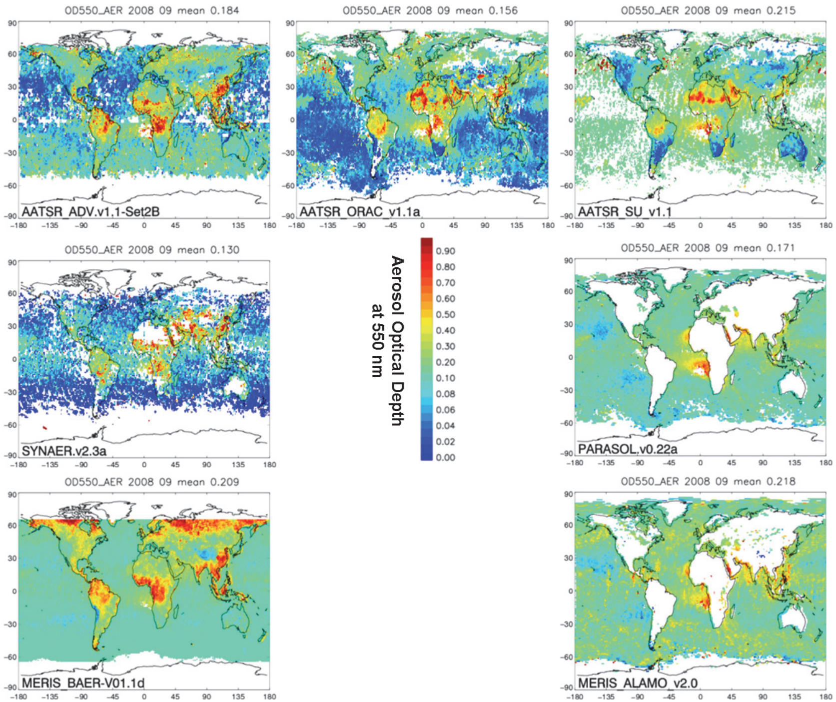

Fig. 7. September 2008 unweighted monthly mean AOD550 for seven total column precursor algorithms as in Fig. 6: datasets with use of common aerosol components and (partly) free retrieval (experiment number 1 in Table 3).

AMTD
6, 2353–2411, 2013

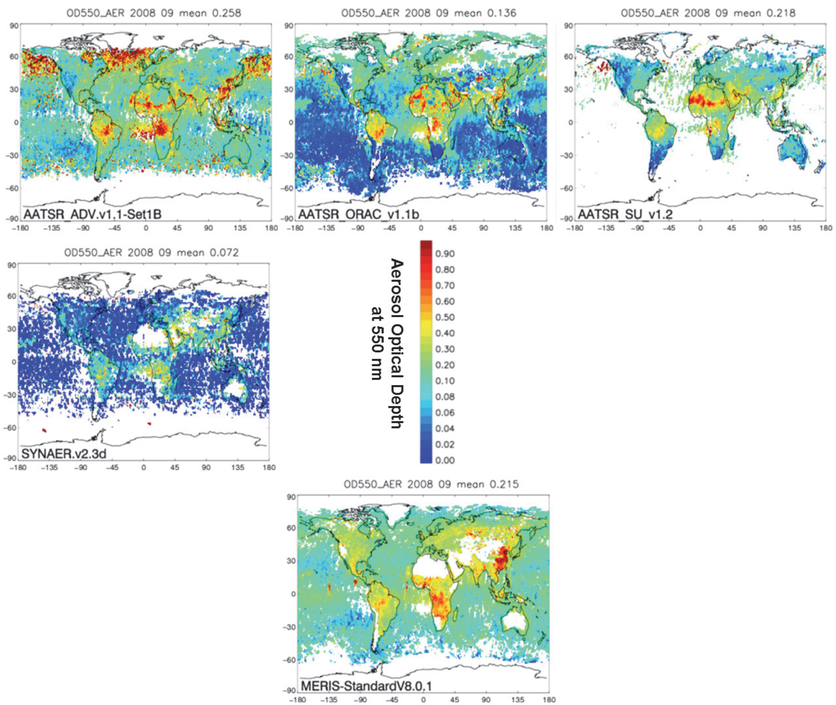

Fig. 8. September 2008 unweighted monthly mean AOD550 for five total column precursor algorithms as in Fig. 6: datasets with use of common aerosol components and AeroCom/AERONET climatology as prescription or a priori information (experiment number 2 in Table 3).

AMTD
6, 2353–2411, 2013

Aerosol retrieval experiments in the ESA Aerosol_cci project

T. Holzer-Popp et al.

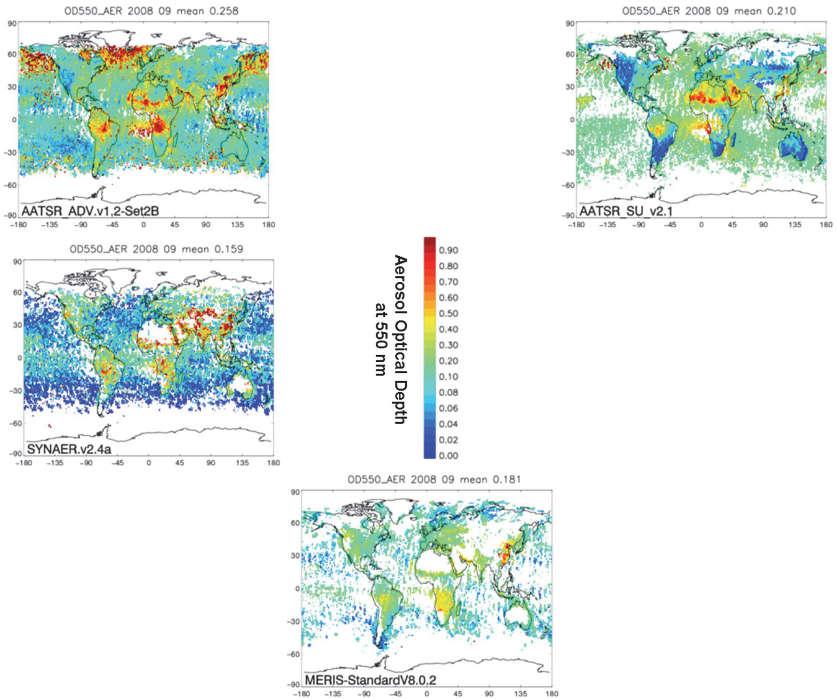

Fig. 9. September 2008 unweighted monthly mean AOD550 for four total column precursor algorithms as in Fig. 6: datasets with use of common aerosol components and (partly) free retrieval or AeroCom/AERONET climatology as a priori information and common cloud mask (experiment number 3 in Table 3).

AMTD
6, 2353–2411, 2013

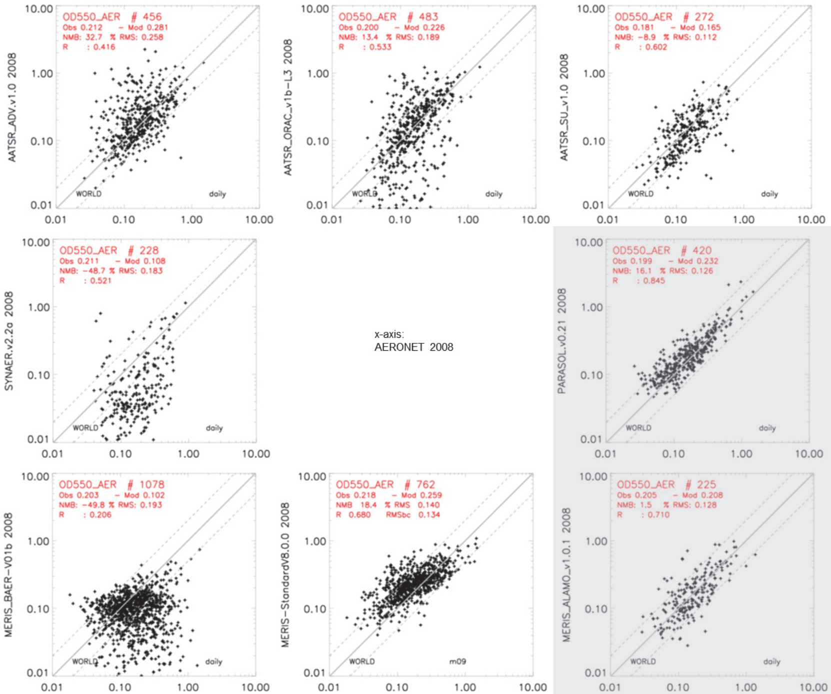

Fig. 10. Scatter plots for September 2008 daily AOD550 versus AERONET for eight total column precursor algorithms (baseline versions) as in Fig. 6. Plots shaded in grey refer to results for experiments/algorithms only over ocean.

AMTD
6, 2353–2411, 2013

Aerosol retrieval experiments in the ESA Aerosol_cci project

T. Holzer-Popp et al.

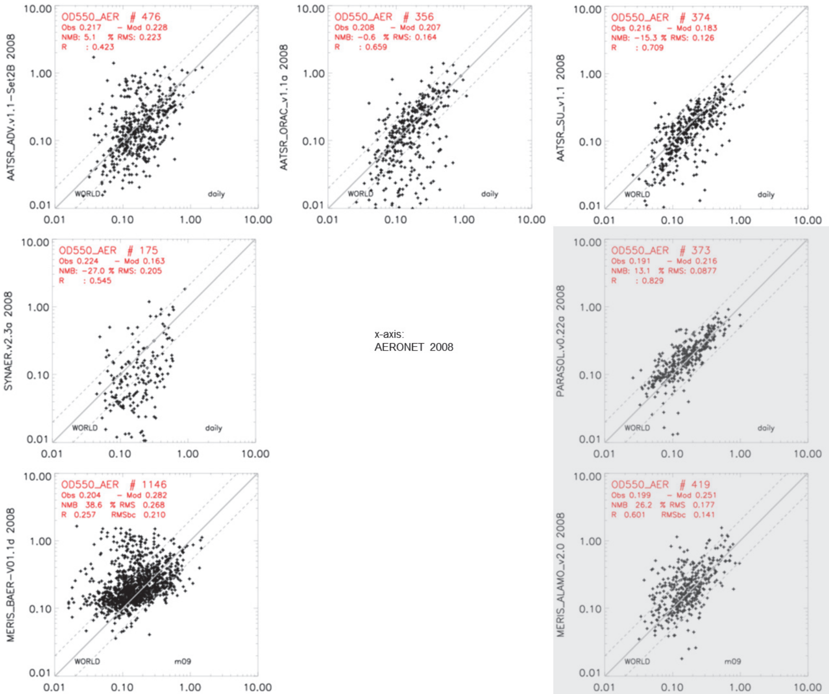

Fig. 11. Scatter plots for September 2008 daily ADO550 versus AERONET for seven total column algorithms using common optical aerosol components as in Fig. 7. Plots shaded in grey refer to results for experiments/algorithms only over ocean.

AMTD
6, 2353–2411, 2013

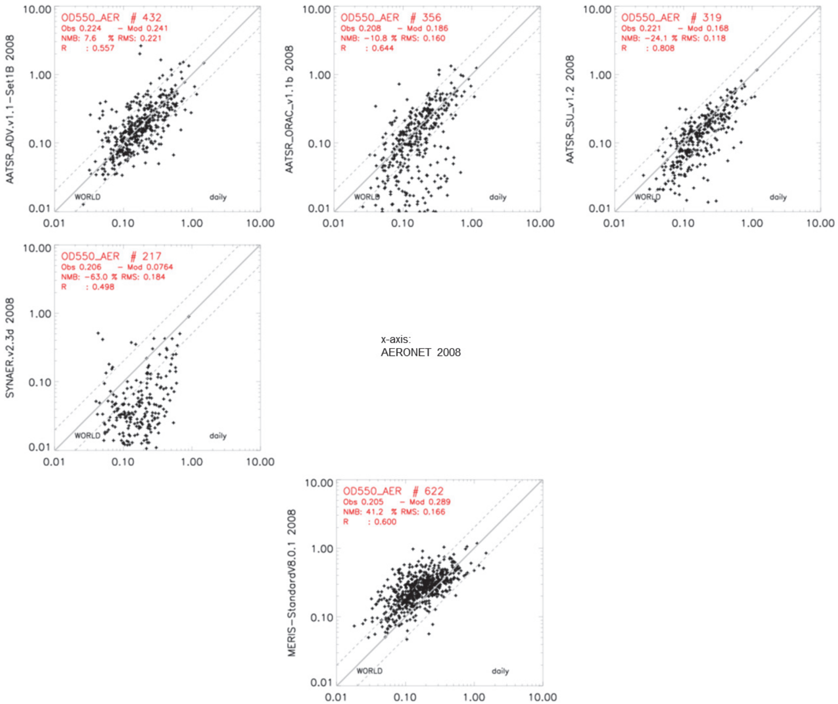

Fig. 12. Scatter plots for September 2008 daily AOD550 versus AERONET for five total column algorithms using a priori aerosol type climatology as in Fig. 8.

AMTD
6, 2353–2411, 2013

Aerosol retrieval experiments in the ESA Aerosol_cci project

T. Holzer-Popp et al.

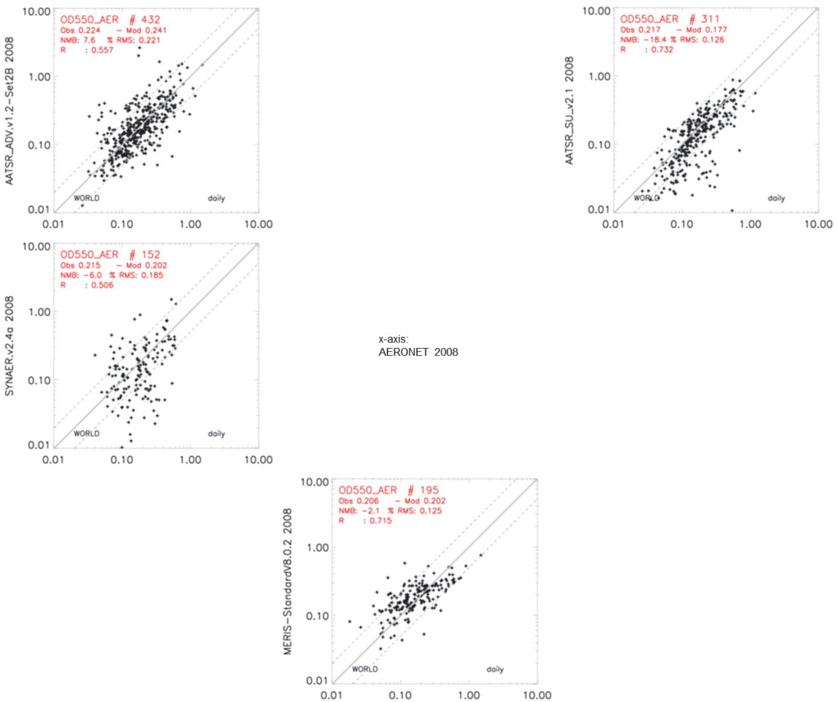

Fig. 13. Scatter plots for September 2008 daily ADO550 versus AERONET for four total column algorithms using a common nadir cloud mask as in Fig. 9.

AMTD
6, 2353–2411, 2013

Title Page
Abstract | Introduction
Conclusions | References
Tables | Figures
◀| |▶
◀ ▶
Back | Close
Full Screen / Esc
Printer-friendly Version
Interactive Discussion

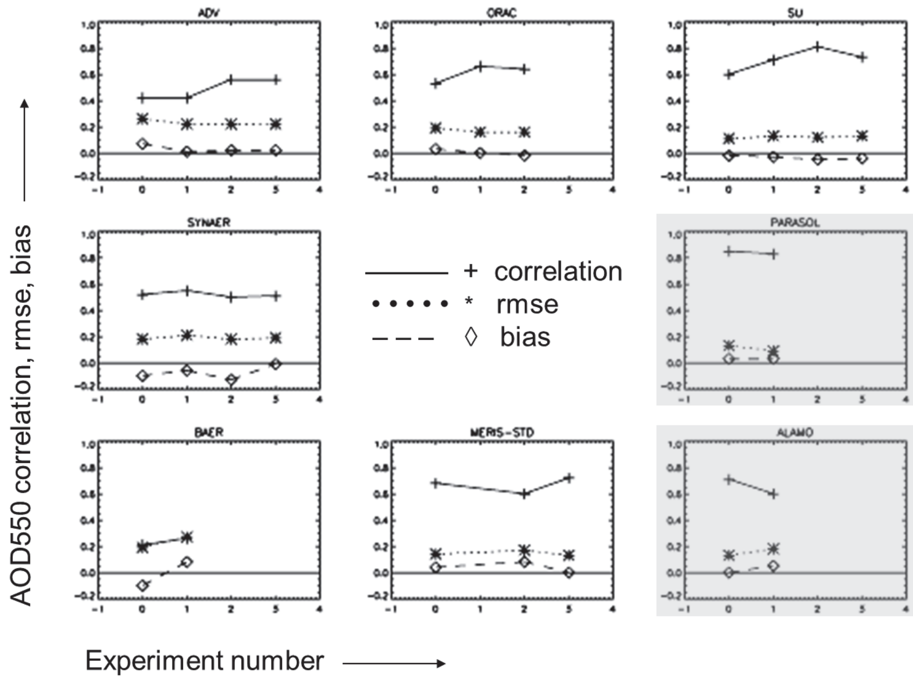

Fig. 14. Evaluation results for the different algorithms and experiments. Each plot shows from top to bottom correlation, rmse and bias. The x-axis gives the number of the respective experiment as defined in Table 3. Each plot provides results for one individual algorithm. Plots shaded in grey refer to results for experiments/algorithms only over ocean.

AMTD
6, 2353–2411, 2013